

1 **Does the GPM mission improve the systematic error component in satellite**
2 **rainfall estimates over TRMM? An evaluation at a pan-India scale**

3 Harsh Beria^{1,2}, Trushnamayee Nanda¹, Deepak Singh Bisht¹, Chandranath Chatterjee¹

4 ¹Agricultural and Food Engineering Department, Indian Institute of Technology Kharagpur,
5 Kharagpur, India

6 ²Institute of Earth Surface Dynamics, University of Lausanne, Switzerland

7 *Correspondence to:* Harsh Beria (harsh.beria93@gmail.com)

8 **Abstract.** Last couple of decades have seen the outburst of a number of satellite based
9 precipitation products with Tropical Rainfall Measuring Mission (TRMM) as the most widely
10 used for hydrologic applications. Transition of TRMM into Global Precipitation Mission
11 (GPM) promises enhanced spatio-temporal resolution along with upgrades in sensors and
12 rainfall estimation techniques. Dependence of systematic error components in rainfall
13 estimates of Integrated Multi-satellitE Retrievals for GPM (IMERG), and their variation with
14 climatology and topography, was evaluated over 86 basins in India for year 2014 and
15 compared with the corresponding (2014) and retrospective (1998-2013) TRMM estimates.
16 IMERG outperformed TRMM for all rainfall intensities across a majority of Indian basins,
17 with significant improvement in low rainfall estimates showing smaller negative biases in 75
18 out of 86 basins. Low rainfall estimates in TRMM showed a systematic dependence on basin
19 climatology, with significant overprediction in semi-arid basins which gradually improved in
20 the higher rainfall basins. Medium and high rainfall estimates of TRMM exhibited a strong
21 dependence on basin topography, with declining skill in higher elevation basins. Systematic
22 dependence of error components on basin climatology and topography was reduced in
23 IMERG, especially in terms of topography. Rainfall-runoff modeling using Variable
24 Infiltration Capacity (VIC) model over a flood prone basin (Mahanadi) revealed that
25 improvement in rainfall estimates in IMERG didn't translate into improvement in runoff
26 simulations. More studies are required over basins in different hydro-climatic zones to
27 evaluate the hydrologic significance of IMERG.

28 **Keywords:** GPM, IMERG, TRMM, VIC, climatology, topography

29 **1 Introduction**

30 The developing part of the world suffers from acute data shortage, both in terms of
31 quality and quantity. A recent commentary from Mujumdar (2015) provided insights into the
32 problems faced by the Indian hydrologic community due to the lack of willingness of the
33 relevant governmental bodies to openly share meteorologic and hydrologic data and its meta
34 data to the research community. With the threats of climate changing looming large, high
35 quality precipitation products (in terms of accuracy, spatial and temporal resolution) are the
36 need of the hour. Satellite precipitation products offer a viable alternative to gauge based
37 rainfall estimates.

38 A number of satellite based precipitation estimates have cropped up in the past two
39 decades, the famous ones being Climate Prediction Center morphing technique (CMORPH),
40 Precipitation Estimation from Remotely Sensed Information Using Artificial Neural
41 Networks (PERSIANN), PERSIANN Climate Data Record (PERSIANN-CDR), Tropical
42 Rainfall Measuring Mission (TRMM), Asian Precipitation - Highly-Resolved Observational
43 Data Integration Towards Evaluation (APHRODITE) and National Oceanic and Atmospheric
44 Administration (NOAA) Climate Prediction Center (CPC). A number of studies over the past
45 decade have evaluated the hydrologic application of these datasets over regions with varied
46 topography and climatology.

47 Artan et al. (2007) found reasonable streamflow simulations using CPC over four
48 basins in Africa and South-east Asia while Collischonn et al. (2008) found similar results
49 using TRMM over Amazon River basin. Akhtar et al. (2009) used neural networks to forecast
50 discharges at varying lead times using TRMM 3B42V6 precipitation estimates. Wu et al.
51 (2012) used TRMM 3B42V6 estimates to develop a real-time flood monitoring system and
52 concluded that the probability of detection (POD) improved with longer flood durations and
53 larger affected areas. Kneis et al. (2014) evaluated TRMM 3B42-V7 and its real-time
54 counterpart TRMM 3B42-V7RT over Mahanadi River basin in India and found the research
55 product (3B42) to be superior to the real-time alternative (3B42RT). Peng et al. (2014) found
56 a systematic dependence of TRMM estimates on climatology in North-West China,
57 characterizing the wetter regions better than the drier ones. Bajracharya et al. (2014) used
58 CPC to drive a hydrologic model over Bagmati basin in Nepal and reported that the
59 incorporation of local rain gauge data tremendously benefited the streamflow simulations.
60 Shah and Mishra (2015) explored uncertainty in the estimates of multiple satellite rainfall

61 products over major Indian basins. Most of the studies which evaluated multiple satellite
62 precipitation estimates have reported TRMM to give the best estimate over the Tropical part
63 of the world (Gao and Liu, 2013; Prakash et al., 2016b; Zhu et al., 2016).

64 Tropical Rainfall Measuring Mission (TRMM) satellite was launched in late 1997 and
65 provides high resolution ($0.25^\circ \times 0.25^\circ$) quasi-global (50° N-S) rainfall estimates (Huffman et
66 al., 2007). The TRMM mission is a joint mission between the National Aeronautics and
67 Space Administration (NASA) and the Japan Aerospace Exploration (JAXA) Agency to
68 study rainfall for weather and climate research. The TRMM satellite produced 17 years of
69 valuable precipitation data over the Tropics.

70 Owing to the tremendous success of TMPA mission, Global Precipitation
71 Measurement (GPM) was launched on February 27, 2014 (Liu, 2016). The GPM sensors
72 carry first spaceborne dual-frequency phased array precipitation radar (DPR) operating at Ku
73 (13 GHz) and Ka (35 GHz) bands and a canonical-scanning multichannel (10 - 183 GHz)
74 microwave imager (GMI) (Hou et al., 2014). The improved sensitivity of Ku and Ka bands
75 allow for improved detection of low precipitation rates (<0.5 mm/h) and falling snow.

76 A few preliminary assessments of GPM over India and China (Prakash et al., 2016a,
77 2016b; Tang et al., 2016a) suggest an improvement over TMPA. For 2014 monsoon (Prakash
78 et al., 2016b) reported that Integrated Multi-satellitE Retrievals for GPM (IMERG), which is
79 a level three multi-satellite precipitation algorithm of GPM (Hou et al., 2014), outperformed
80 TMPA in extreme rainfall detection along the Himalayan foothills in North India and over
81 North Western India, with slightly reduced false alarms. Tang et al. (2016a) found that
82 IMERG outperformed TMPA in almost all the indices for every sub-region of mainland
83 China at 3-hourly and daily temporal resolutions. They also reported that IMERG reproduced
84 probability density functions more accurately at various precipitation intensities and better
85 represented the precipitation diurnal cycles. In another work by Prakash et al. (2016a),
86 IMERG was compared with Global Satellite Mapping of Precipitation (GSMaP) V6 and
87 TMPA 3B42V7 for the 2014 monsoon over India. It was found that IMERG estimates
88 represented the mean monsoon rainfall and its variability more realistically, with fewer
89 missed and false precipitation bias and improvements in the precipitation distribution over
90 low rainfall rates.

91 Most of the previous studies that compared satellite and reanalysis precipitation
92 products for pan-India focused at a grid scale, rather than a basin scale (Prakash et al., 2015,

93 2016a, 2016b). We focused at a basin scale as it is more relevant in terms of water resources
94 assessment for policy makers. It provides a clear signal of the utility of the satellite
95 precipitation products at the required spatial resolution for water managers working at a basin
96 scale. Also, at a basin scale, the statistical and hydrologic results are more complementary
97 (Bisht et al., 2017; Kneis et al., 2014).

98 In this study, we comprehensively evaluated TRMM 3B42 from 1998-2013 over 86
99 basins in India and explored systematic biases due to climatology and topography. We then
100 compared TRMM 3B42 precipitation estimates with IMERG for 2014 and explored if the
101 systematic biases were reduced in IMERG, and whether IMERG was able to better capture
102 the low rainfall magnitudes. Finally, we used a macroscale hydrologic model (Variable
103 Infiltration Capacity (VIC)) to evaluate TRMM and IMERG over a flood prone basin in
104 Eastern India (Mahanadi River basin) for the year 2014.

105 **2 Description of the study area, datasets used and methodology**

106 **2.1 Study area**

107 Water Resources Information System of India (India-WRIS) delineates India into
108 multiple sub-basins (Fig. 1a) (India, 2014). In this study, 86 basins were used, with the five
109 excluded basins located in the Jammu and Kashmir region of Northern India (details included
110 in Supplementary table 1). Also, the Lakshadweep islands (located off the Indian West coast
111 in the Arabian Sea) and the Andaman and Nicobar islands (located in the Bay of Bengal)
112 were excluded from the analysis due to scarce rain-gauge monitoring network.

113 Most of India experiences a tropical monsoon type of climate receiving an average
114 annual rainfall of around 1100 mm/year, of which about 70-80% is concentrated during the
115 monsoon season (June – September). Fig. 2a shows the spatial distribution of rainfall (details
116 in supplementary table 1), calculated using India Meteorological Department (IMD) gridded
117 precipitation dataset (computed using 31 years (1980-2010) of rainfall time series) over India.
118 The Western Ghats (located on the Indian West coast) and the North-Eastern basins receive
119 the highest rainfall, with magnitudes going up to 3000 mm/year. The Western Ghats receive
120 orographic rainfall due to steep topographic gradient that exist from the West to the East,
121 making the Eastern part a leeward area where rainfall is mainly associated with the passage
122 of lows and depressions developed in the Bay of Bengal (Prakash et al., 2016a). Details of the
123 orographic features of rainfall over Western Ghats can be found in Tawde and Singh (2015).

124 The high rainfall in the North-Eastern part of India is associated with orographic control and
125 multi-scale interactions of monsoon flow (Prakash et al., 2016a). Basins in the Indo-Gangetic
126 plain and on the East coast receive above average rainfall of around 1400 mm/year, governed
127 by the tropical monsoons. The North-west basins, associated with semi-arid type of climate,
128 receive low annual rainfall ranging from 300-400 mm/year.

129 Fig. 2b shows the spatial distribution of the basin-wise elevation above mean sea level
130 (m.s.l) (details in supplementary table 1). The Northern tract of Jammu and Kashmir
131 comprises the basins with highest elevations, in between 2500 m to 5000 m above m.s.l.
132 These basins suffer from scarce rain monitoring networks, due to which five of these high
133 elevation basins have been ignored in the analysis. High Pitch Mountains are also found in
134 the North-Eastern basins where basin-wise elevation goes as high as 1400 m above m.s.l. The
135 Western Ghats are characterized by a sharp topographic gradient with the elevations
136 increasing from around 200 m on the West coast to above 600 m above m.s.l as we move
137 east. This transition results in heavy orographic rainfall on the West coast and leads to the
138 sharp rainfall contrast on the leeward side of the Western Ghats.

139 Rainfall-runoff modeling was done in Hirakud catchment of the Mahanadi River
140 basin (MRB) and Wainganga catchment of Godavari River basin. MRB, situated on the
141 Eastern coast of India, is one of the largest Indian basins draining an area of 1,41,000 km². It
142 is prone to frequent flooding at the downstream, with five major flood events in the first
143 decade of the 21st century (Jena et al., 2014). On the upstream of the MRB is a multi-purpose
144 dam (Hirakud) which encompasses catchment area of around 85,200 km² (Fig. 1b). Hirakud
145 dam started its operations in 1957 and its upstream does not include any major dam, although
146 a number of small scale irrigation reservoirs are operational during the monsoon.
147 Agricultural, forest and shrub land account for around 55%, 35% and 7% of the total basin
148 coverage respectively (Kneis et al., 2014). Wainganga river basin, the largest sub-basin of
149 Godavari basin (located in Peninsular India) drains a total of 51,422 km² area. Both the
150 basins receive annual rainfall of around 1500 mm.

151 **2.2 Datasets used**

152 IMD gridded rainfall dataset was used as the reference product and Tropical Rainfall
153 Measuring Mission (TRMM) and Integrated Multi-satellitE Retrievals for GPM (IMERG)
154 were compared against IMD. A brief summary of the datasets is given in Table 1. A brief
155 introduction to the three rainfall datasets is given below.

156 **2.2.1 Gridded IMD and streamflow dataset**

157 IMD gridded precipitation dataset provides daily rainfall estimates over the Indian
158 landmass from 1901-2014 at a spatial resolution of $0.25^\circ \times 0.25^\circ$. It has been developed using
159 a dense network of rain gauges consisting of 6955 stations and is known to reasonably
160 capture the heavy orographic rainfall in the Western Ghats, the Northeast and the low rainfall
161 on the leeward side of the Western Ghats. Details about the number of stations used to make
162 the gridded product are discussed in the supplementary material. For a detailed discussion on
163 the evolution of IMD gridded dataset, refer to Pai et al. (2014).

164 It is to be noted that IMD measures rainfall accumulation at 8:30 AM Indian Standard
165 time (IST) or (3:00 AM UTC). The accumulated rainfall for the previous day is provided as
166 the rainfall estimate for current day. For instance, IMD rainfall estimate at a gauging station
167 for September 14th, 2014 refers to the rainfall accumulation from 8:30 AM IST (3:00 AM
168 UTC) on September 13th, 2014 to 8:30 AM IST (3:00 AM UTC) on September 14th, 2014.
169 Both TRMM and IMERG precipitation estimates were converted to IMD timescale.

170 The gridded daily minimum and maximum temperature was obtained from IMD at a
171 spatial resolution of $1^\circ \times 1^\circ$ (Srivastava et al., 2009). Daily wind speed data was obtained
172 from coupled National Centers for Environmental Prediction (NCEP) and Climate Forecast
173 System Reanalysis (CFSR) at a spatial resolution of $0.5^\circ \times 0.5^\circ$. Daily discharge data at the
174 inflow site of the Hirakud reservoir was obtained from the State Water Resources Department
175 (Odisha), Hirakud Dam Project, Burla, Sambalpur. Daily discharge data at Wainganga basin
176 was obtained through WRIS-website (<http://www.india-wris.nrsc.gov.in/wris.html>).

177 **2.2.2 Tropical Rainfall Measuring Mission (TRMM)**

178 In order to provide high resolution precipitation dataset in real-time, the TRMM
179 satellite was launched in late 1997 and it provides 3-hourly rainfall estimates from 1998 to
180 the current date at a quasi-global coverage (50° N-S) at a spatial resolution of $0.25^\circ \times 0.25^\circ$
181 (Huffman et al., 2007). Two variants of TRMM multi-satellite precipitation analysis (TMPA)
182 are available, a real time product which is available at 3-6 hours latency and the research
183 product which is available at 2-months latency. TRMM research product makes use of rain
184 gauge stations from Global Precipitation Climatology Centre (GPCC) to post-process the
185 TRMM estimates, details of which can be found in Huffman et al. (2007). We used TRMM
186 research product in this study (henceforth mentioned as TRMM).

187 **2.2.3 Integrated Multi-Satellite Retrievals for GPM (IMERG)**

188 IMERG is the day-1 multi-satellite precipitation algorithm for GPM which combines
189 data from TMPA, PERSIANN, CMORPH and NASA PPS (Precipitation Processing
190 System). For a detailed understanding of the retrieval algorithm of IMERG, refer to
191 (Huffman et al., 2014; Liu, 2016).

192 The major advancement in GPM satellite is the improved sensitivity of sensors
193 leading to improved detection of low precipitation rates (<0.5 mm/h) and falling snow, a
194 known shortcoming of TRMM. IMERG is available in 3 variants, (a) Early run (latency ~ 6
195 hours), (b) Late run (latency ~ 18 hours) and (c) Final run (latency ~ 4 months) (Liu, 2016).
196 Each product is available at half-hourly temporal and $0.1^\circ \times 0.1^\circ$ spatial resolution. The
197 spatial coverage is 60° N-S which is planned to be extended to 90° N-S in the near future. We
198 used the Final run product in our analysis.

199 **2.3 VIC Hydrological Model**

200 VIC is a macroscale semi-distributed hydrological model which uses a grid-based
201 approach to quantify different hydro-meteorological processes by solving water balance and
202 energy flux equations, specifically designed to represent the surface energy and hydrologic
203 fluxes at varying scales (Liang et al., 1994, 1996). VIC uses multiple soil layers with variable
204 infiltration, non-linear baseflow and addresses the sub-grid scale variability in vegetation. A
205 stand-alone routing model (Lohmann et al., 1996) is used to generate runoff and baseflow at
206 the outlet of each grid cell, assuming linear and time-invariant runoff transport. The land
207 surface parameterization (LSP) of VIC is coupled with a routing scheme in which the
208 drainage system is conceptualized by connected-stem rivers at a grid scale. The routing
209 model extends the FDTF-ERUHDIT (First Differenced Transfer Function-Excess Rainfall
210 and Unit Hydrograph by a Deconvolution Iterative Technique) approach (Duband et al.,
211 1993) with a time scale separation and liberalized Saint-Venant equation type river routing
212 model. The model assumes runoff transport process to be linear, stable and time invariant.

213 VIC has been successfully used in a number of global and local hydrologic studies
214 (Hamlet and Lettenmaier, 1999; Shah and Mishra, 2016; Tong et al., 2014; Wu et al., 2014;
215 Yong et al., 2012). A recent commentary on the need for process-based evaluation of large-
216 scale hyper-resolution models by Melsen et al. (2016) provides interesting insights into the
217 use of VIC at different spatial scales and why we shouldn't just decrease the grid size (hence

218 increasing the spatial resolution of model) without considering the dominant processes at that
219 scale. In lines with the discussions in Melsen et al. (2016), VIC was run at a grid size of 0.5°
220 $\times 0.5^\circ$ for Hirakud basin and at $0.25^\circ \times 0.25^\circ$ for Wainganga basin.

221 **2.4 Methodology**

222 All the analysis was performed at a basin scale. Basin-wise mean areal rainfall was
223 calculated for all the three rainfall products (IMD, TRMM and IMERG) using Thiessen
224 Polygon method for their respective periods of availability.

225 In order to statistically evaluate the precipitation products, two skill measures were
226 used (Pearson correlation (R) and percentage bias (Pbias/bias)) along with two threshold
227 statistics (probability of detection (POD) and false alarm ratio (FAR)). Table 2 shows the
228 contingency table and Table 3 provides a summary of the statistical indices.

229 All the statistical inferences were drawn for the overall time series, and then
230 separately for the different rainfall regimes. Table 4 shows the criterion to segregate the
231 rainfall time series into different components. For computing POD and FAR for different
232 rainfall regime, a threshold is required. The 25th percentile value was selected as the
233 threshold for low rainfall regime, 50th percentile for medium regime, 75th percentile for high
234 rainfall regime and 95th percentile for very high rainfall regime. The statistical indices were
235 calculated basin-wise.

236 In order to identify systematic bias in the satellite products, one meteorologic index
237 (long term basin mean annual rainfall) and one topographic index (basin mean elevation) was
238 computed for the 86 basins. The long term mean annual rainfall was computed using IMD
239 gridded dataset from 1980 – 2010 (31 years). Basin mean digital elevation model (DEM) was
240 extracted from Shuttle Radar Topography Mission (SRTM) DEM and mean elevation was
241 obtained on a basin-wise scale.

242 Due to the limited availability of IMERG data (starting from 2014), calibration of
243 VIC was done using an approach similar to the one used by Tang et al. (2016b). First, VIC
244 was calibrated (2000-2011) and validated (2011-2014) using gridded IMD precipitation time
245 series. VIC was then calibrated (2000-2011) and validated (2011-2014) with TRMM
246 precipitation time series. Further, both the IMD and TRMM calibrated models were validated
247 with IMERG and TRMM for the year 2014 (from April 1, 2014 to December 31st, 2014).
248 The year 2000 was used as a warm up period for the model.

249 In line with the recent discussion by McCuen (2016) on the correct usage of statistical
250 and graphical indices to evaluate model calibration and validation, four statistical parameters
251 (Nash Sutcliffe efficiency (NSE), Percentage bias (Pbias), coefficient of determination (R^2)
252 and root mean squared error (RMSE)) were used to evaluate the runoff simulations from
253 VIC. Table 3 provides a summary of these indices.

254 **3 Results**

255 All the TRMM statistics were obtained for two distinct periods (1998-2013 and
256 2014). For the year 2014, the IMERG precipitation estimates were available from March 12,
257 2014. Therefore, the TRMM statistics for the year 2014 were obtained from March 12, 2014
258 to December 31, 2014. Henceforth, for the sake of convenience, statistics of TRMM-R refers
259 to the time period 1998-2013, statistics of TRMM and IMERG refers to the time period
260 March 12, 2014 to December 31, 2014.

261 **3.1 Scatterplots**

262 Fig. 3 shows the scatterplot of IMERG and TRMM with respect to IMD precipitation
263 combining data from all the 86 basins for the year 2014. IMERG shows better correlation in
264 60 out of 86 basins. On looking at the scatterplots for individual basins (Fig. 4), IMERG
265 tends to be better correlated to IMD than TRMM. It can be seen that the correlation values go
266 as high as 0.96 for IMERG (and 0.94 for TRMM) with a very uniform spread across the 1:1
267 line for the five best basins (Figs. 4a–e) (decided on the basis of correlation of IMERG with
268 IMD in 2014). These basins are situated in the flat Deccan Plateau belt in South-central India
269 (mostly concentrated in Tapi and Godavari basins). For the other five basins (Figs. 4f–j), the
270 poor correlation is due to the gross overestimation of IMERG/TRMM over IMD. Four of
271 these five basins are situated in the high elevation basins in Northern India, which hints at a
272 systematic dependence of IMERG/TRMM estimates with elevation. This is explored in detail
273 in section 3.5.

274 **3.2 Basin-wise correlation**

275 Basin-wise correlation was computed for retrospective analysis of TRMM-R and to
276 compare TRMM and IMERG rainfall estimates for the year 2014. Table 5 provides the
277 summary of the number of basins where IMERG/TRMM has a higher correlation. IMERG
278 gives better rainfall estimates in majority of basins for all rainfall regime. The decomposition

279 of the overall time series into different rainfall regime reduces the correlation, which can be
280 attributed to temporal smoothing in longer time series.

281 The spatial maps (Fig. 5) provide an illustration of the slight improvement of IMERG
282 over TRMM with spatially coherent patterns. In the overall spatial maps (Figs. 5b–c), for the
283 year 2014, TRMM and IMERG show similar skill, with IMERG capturing the rainfall
284 slightly better in Central and Southern India. Both show similar skill in the high rainfall areas
285 of the Western Ghats and the North Eastern basins. IMERG gives slightly better estimates in
286 the high elevation basins in North India. There is no significant improvement in the basins
287 located on the Eastern coast (like the Mahanadi river basin). TRMM provides slightly better
288 estimates of rainfall in the semi-arid basins located in the North Western states of India
289 (Rajasthan). It is to be noted that TRMM statistics for 2014 are much better than its
290 retrospective statistics (TRMM-R) with spatial coherent trends.

291 The low rainfall estimates (Figs. 5d–f) over the semi-arid North Western basins are
292 slightly better for TRMM compared to IMERG. IMERG captures low rainfall better over the
293 Indo-Gangetic plain. Both IMERG and TRMM show similar trends over the Western Ghats,
294 North-Eastern basins, Eastern coast and over the Deccan Plateau. IMERG doesn't capture the
295 low rainfall regime over the Upper Indus basin (in Northern India) and over the upper Bhima
296 and the upper Godavari basin (in the Deccan plateau belt).

297 The medium rainfall estimates (Figs. 5g–i) are best represented in Central India and
298 over the Deccan Plateau by TRMM and IMERG. Both show similar statistics over the
299 Western Ghats and basins in North-Eastern and Eastern coast of India. TRMM slightly
300 outperforms IMERG in the North-Western basin of Rajasthan, a trend also found in the low
301 rainfall regime. IMERG doesn't capture the medium rainfall trends over the Upper Indus
302 basin (in Northern India). In general, TRMM-R medium rainfall estimates are best correlated
303 in the semi-arid region of Rajasthan (North-Western basins) and in Central India. There is not
304 much variability in the correlation of medium rainfall trends of TRMM-R, with correlation
305 coefficient mostly around 0.5 for entire India, except for the high elevation Upper Indus
306 basin.

307 The high rainfall estimates (Figs. 5j–k) show highest correlation in the Deccan
308 Plateau belt, higher elevation basins in Northern India, the Western Ghats and the East coast
309 basins (except for the Southern-most basin) for TRMM and IMERG. High rainfall estimates
310 of TRMM are better correlated than IMERG in the North-Eastern basins of Brahmaputra and

311 Barak and the North-Western basins of Rajasthan. Both show similar correlation over the
312 high elevation basins in the North and over the Western Ghats. IMERG outperforms TRMM
313 in the rain-shadow area of the Western Ghats and in the South-Eastern basins of Pennar and
314 Cauvery. Retrospective maps of TRMM-R (Fig. 5j) suggest that high rainfall is adequately
315 captured in the Indo-Gangetic plain, Western Ghats, North-Western basins of Rajasthan,
316 South-Eastern basins of Pennar and Cauvery and the Eastern coast basins of Central India.
317 However, TRMM gives very low correlation values for the rain-shadow belt of the Western
318 Ghats, suggesting that it doesn't capture the steep orographic gradient. The high rainfall
319 estimates of TRMM-R give modest correlation in the North-Eastern basins, high elevation
320 basins in Northern India and the West most basins of the South (Varrar and Periyar).

321 **3.3 Basin-wise bias**

322 Basin-wise bias was computed for retrospective analysis of TRMM-R and to compare
323 TRMM and IMERG rainfall estimates for the year 2014. Bias for low rainfall regime (Fig.
324 S2b) suggests that TRMM is more positively biased than IMERG for 75 out of 86 basins
325 implying overestimation, which is a known problem with TRMM as its sensors cannot detect
326 very low rainfall magnitudes (<0.5 mm/hour) (Hou et al., 2014). If it detects a low intensity
327 storm, it is most likely to overestimate (Fig. S2b). This seems to have improved in the
328 IMERG product, due to the sensor improvements in the GPM mission (Huffman et al., 2014).
329 The number of unbiased basins ($-10\% \leq \text{bias} \leq 10\%$) increased from 28 in TRMM to 37 in
330 IMERG basins.

331 The spatial maps for the overall rainfall time series (Figs. 6a-c) suggests similar bias
332 patterns in TRMM and IMERG with spatial coherent trends throughout most of India.
333 IMERG gives slightly smaller bias (closer to zero) over the high elevation basins of North
334 India (Upper Indus basin) and slightly larger bias (more negative) over the North Eastern
335 basins (of Brahmaputra and Barak) and the West flowing rivers of Kutch on the Western
336 coast in the state of Gujarat. IMERG and TRMM give large positive biases (overprediction)
337 over Upper and Middle Godavari basin (in Deccan Plateau belt) which suggests that the sharp
338 topographic gradient is not well captured. Retrospective maps of TRMM-R suggest
339 underestimation over high elevation basins in Northern India (Indus, Jhelum and Chenab
340 basins). However, TRMM captures the heavy precipitation on the Western Ghats well with
341 low biases.

342 The low rainfall spatial maps (Figs. 6d–f) show large overprediction (positive bias) by
343 TRMM (1998-2013 and 2014) which is improved in IMERG. The improvement is most
344 prominent in the North Eastern basins (of Brahmaputra and Barak), Central India (Mahi,
345 Chambal and the Indo-Gangetic plain), rain-shadow area of the Western Ghats and the South-
346 Eastern coast. IMERG shows gross overprediction over Luni basin (near the Western coast of
347 Rajasthan). Retrospective TRMM-R maps for low rainfall regime (Fig. 6d) show that the low
348 rainfall was best captured in high rainfall areas of the Western Ghats, the Indo-Gangetic plain
349 and the Eastern coastal basins, which is not very surprising as TRMM doesn't detect low
350 rainfall magnitudes very well, thus suffering from overprediction in arid and semi-arid basins.
351 Improvement in the low rainfall sensors in IMERG has improved low rainfall estimates, but it
352 still suffers from gross overprediction in semi-arid areas (as evident in the semi-arid basins in
353 North-West India (Fig. 6f)).

354 The medium rainfall spatial maps (Figs. 6g–i) suggest similar spatial bias pattern in
355 TRMM and IMERG. Both TRMM and IMERG suffer from underprediction (negative bias)
356 in the high elevation Northern basins (of Indus and Jhelum), although IMERG seem to be less
357 biased than TRMM. Both show similar trends in the Western Ghats, with low bias. However,
358 both the products show large positive bias (overprediction) in the Middle Godavari basin,
359 unable to capture the sharp topographic gradient in the region. IMERG slightly overpredicts
360 rainfall in the North Eastern basins (of Brahmaputra and Barak). The retrospective TRMM
361 maps for medium rainfall (Fig. 6g) show low bias over entire India, except over the Western
362 Ghats (slight underprediction) and high elevation Northern basins of Indus and Jhelum
363 (strong underprediction).

364 The high rainfall spatial maps (Figs. 6j–l) suggest similar spatial pattern in TRMM
365 and IMERG, with slight negative bias over majority of the basins. The high rainfall in the
366 Western Ghats is well represented in TRMM and IMERG, however with strong
367 overprediction in the leeward side of the Western Ghats, suggesting that IMERG is unable to
368 capture the sharp topographic gradients. IMERG shows greater underprediction in the high
369 rainfall areas of the North Eastern basins than TRMM, however giving better estimates in the
370 high elevation basins in Northern India. Both IMERG and TRMM give similar bias pattern in
371 the Indo-Gangetic plain and the semi-arid areas of the North-West. The retrospective
372 TRMM-R map of high rainfall (Fig. 6j) suggests spatially homogeneous trends throughout
373 India. However, it suffers from gross underestimation in the high elevation basins of
374 Northern India (Indus, Jhelum and Chenab). It is clearly observed that the high elevation

375 basins are an outlier in most of the analysis. A systematic dependence of bias with elevation
376 may be an underlying trend which is further explored in section 3.5.

377 **3.4 Threshold statistics**

378 Increasing rainfall threshold leads to deteriorating trends in POD and FAR across
379 majority of the basins, with decreasing POD and increasing FAR. Table 6 summarizes the
380 number of basins in which IMERG/TRMM gives higher/lower threshold statistics, including
381 the basins in which they show similar results. At low rainfall threshold, IMERG shows major
382 improvement in POD in the Western region of Gujarat (Luni, Bhadar and Setrunji basins)
383 (Figs. 7b,c). The average POD (low rainfall threshold) across basins is 0.95 for IMERG and
384 0.91 for TRMM. At medium rainfall threshold, average POD across basins is 0.87 for both
385 IMERG and TRMM. Notably, IMERG gives lower POD (medium rainfall threshold) in two
386 (Barak and Brahmaputra lower sub-basin) out of the three North-Eastern basins, and higher
387 POD (medium rainfall threshold) in the semi-arid basins of Rajasthan and Gujarat (Luni,
388 Bhadar and Setrunji basins) (Figs. 7e,f). At high rainfall threshold, average POD across
389 basins is 0.76 for IMERG and 0.77 for TRMM. There is notable fall in performance in all the
390 three North-Western basins. IMERG gives slightly higher POD (high rainfall threshold) in
391 the high elevation Northern basins (Upper Indus and Jhelum basins) (Figs. 7h,i). At very high
392 rainfall threshold, average POD across basins is 0.72 for IMERG and 0.7 for TRMM. At very
393 high rainfall threshold, it's clear that POD of IMERG is worse for all the three North-Eastern
394 basins and over the semi-arid basins of Rajasthan and Gujarat (Figs. 7k,i). There is slight
395 improvement in POD values for the high elevation Northern basins (Chenab, Ravi, Beas and
396 Satulaj basins).

397 At low rainfall threshold, the average FAR across basins is 0.24 for TRMM and 0.22
398 for IMERG. At medium rainfall threshold, average FAR across basins is 0.22 for TRMM and
399 0.19 for IMERG. Notably, IMERG outperforms TRMM at low and medium rainfall
400 thresholds giving lower FAR in the Western basins of Gujarat (Luni and Setrunji basins)
401 (Figs. 8b,c,e,f). At high rainfall threshold, average FAR across basins is 0.18 for IMERG and
402 0.22 for TRMM. Slightly reduced FAR are seen in Central India (Yamuna and Chambal
403 basins) and the North-Eastern basins (Brahmaputra basin) in IMERG at high rainfall
404 threshold (Figs. 8h,i). At very high rainfall threshold, average FAR across basins is 0.33 for
405 IMERG and 0.41 for TRMM. There are notably fewer false alarms in IMERG estimates over
406 the Northern, North-Eastern basins and the Western Ghats at very high thresholds. Both

407 products give similar FAR (very high threshold) along the Eastern coast and Deccan Plateau
408 basins.

409 POD for TRMM-R suggests decreasing POD and increasing FAR with increasing
410 rainfall threshold (Figs. 7a,d,g,j, Figs. 8a,d,g,j). The average POD across basins is 0.89, 0.85,
411 0.77 and 0.66 for low, medium, high and very high rainfall thresholds, respectively. The
412 respective FAR values are 0.26, 0.22, 0.21 and 0.43. At high and very high threshold, POD
413 drops significantly over the high elevation Northern basins and high rainfall North-Eastern
414 basins and the Western Ghats) (Figs. 7g,j). High FAR is recorded in the basins in Gujarat
415 (Luni and Setrunji) and Central India (Bhadar and Chambal) at low and medium rainfall
416 threshold (Figs. 8a,d) suggesting TRMM creates a lot of false alarms at low and medium
417 rainfall magnitudes. There is a sharp contrast between FAR at high and very high thresholds,
418 with low FAR at high rainfall threshold (75 percentile) and high FAR at very high threshold
419 (95 percentile) (Figs. 8g,j). This suggests that TRMM-R creates a lot of false alarms at very
420 high rainfall thresholds, especially in the North-Eastern, Northern and extreme Southern
421 basins (Fig 8j).

422 **3.5 Systematic error in satellite estimates as a function of annual rainfall and mean** 423 **elevation**

424 The satellite precipitation estimates were evaluated against a climatologic parameter
425 (long term annual rainfall of basin) and a topographic parameter (basin mean elevation), to
426 investigate if there was any systematic variation in errors with climatology or topography.
427 There is no systematic dependence between the climatologic and topographic parameter ($R =$
428 0.07 , Fig S3) and they can be considered as independent (implying minimal interference).

429 TRMM-R rainfall estimates exhibited very strong dependence on mean basin
430 elevation, with decreasing skill (larger bias and lower correlation) in basins with high mean
431 elevation (Figs. 9 and 10). For medium and high rainfall regimes (Figs. 9c, d), bias values
432 were highly negative for high elevation basins (especially for basins with mean elevation $>$
433 2000 m), implying underprediction. The corresponding correlation values (Figs. 10c, d) also
434 suggested reduced skill at high elevation basins.

435 For the year 2014, the systematic dependence of bias on basin elevation improved in
436 IMERG estimates, with correlation between basin-wise bias and elevation reducing from -
437 0.43 to -0.32 for medium rainfall intensity (Fig. 11c) and from -0.31 to -0.08 for high rainfall

438 intensity (Fig. 11d). The same was not observed in the correlation plots (Fig. 12). At low
439 rainfall intensity (Fig. 12b), IMERG estimates exhibited stronger systematic relationship
440 between basin-wise correlation and elevation, with strongly decreasing correlation with
441 elevation than TRMM. At medium rainfall intensity (Fig. 12c), both TRMM and IMERG
442 showed decreasing skill with increasing elevation. This systematic dependence was stronger
443 in IMERG than TRMM, as reflected in the higher negative correlation between basin-wise
444 correlation and elevation in medium rainfall IMERG estimates (Fig. 12c).

445 The same analysis was repeated against mean annual precipitation (Figs. S4-S7)
446 wherein systematic error dependence was found to be smaller. TRMM-R rainfall estimates
447 exhibited systematic dependence of bias and correlation with basin wise mean annual rainfall
448 for low and medium rainfall estimates (Fig. S4 and S5). At low rainfall intensity, TRMM-R
449 estimates for basins experiencing low annual rainfall were found to be strongly positively
450 biased (Fig. S4b), implying significant over-estimation. For the year 2014, systematic
451 dependence of bias was reduced in IMERG at medium rainfall intensities (Fig. S6c,
452 correlation improved from -0.43 in TRMM to -0.3 for IMERG). A substantial skill was lost in
453 terms of decreasing correlation for basins receiving high rainfall in both TRMM and IMERG
454 estimates (Fig. S7c). At high rainfall intensities, bias was more negative (implying
455 underprediction) in basins which received more rainfall in both IMERG and TRMM (Fig.
456 S6d).

457 **3.6 Rainfall-runoff modeling**

458 Rainfall-runoff modeling was carried out over Hirakud catchment of Mahanadi River
459 basin and Wainganga catchment of Godavari River basin, with the calibration and validation
460 periods as 2000-2011 and 2012-2014, respectively. VIC was first calibrated with IMD
461 gridded precipitation and then with TRMM3B42 V7. The two calibrated models were then
462 forced with TRMM and IMERG precipitation for the year 2014 (April – December). Tables 7
463 and 8 show the model performances.

464 The IMD calibrated model showed better simulations compared to the TRMM
465 calibrated model, with higher NSE, coefficient of determination and smaller bias and RMSE
466 in both Wainganga and Hirakud basins. TRMM calibrated model showed overprediction
467 (positive bias) in Hirakud basin, but was relatively unbiased in Wainganga basin ($-10 \leq$
468 $P_{bias} \leq 10$) (Tables 7, 8).

469 The IMERG simulations with IMD and TRMM calibrated models were slightly
470 inferior in comparison with TRMM simulations for 2014 (NSE = 0.64 for IMERG and 0.72
471 for TRMM in IMD calibration; NSE = 0.7 for IMERG and 0.72 for TRMM in TRMM
472 calibration) (Table 7, Fig. 13) for Hirakud. However, the IMERG simulations gave similar
473 results as TRMM in Wainganga basin when calibrated using IMD data, but inferior results
474 when calibrated with TRMM data (NSE = 0.61 for IMERG and 0.72 for TRMM) (Table 8,
475 Fig. 14). In case of Hirakud basin, IMERG simulations gave higher NSE when calibrated
476 with TRMM data. However, in the case of Wainganga basin, IMERG gave higher NSE when
477 calibrated with IMD data. The high negative bias in IMERG simulations (with IMD and
478 TRMM calibrated models) showed significant overprediction compared to TRMM.

479 Both TRMM and IMERG underestimated the magnitude of the two major peaks (flow
480 $> 15000 \text{ m}^3/\text{s}$) in Hirakud and Wainganga basin in 2014 (Figs. 13, 14). However, the phase
481 was well captured by both IMERG and TRMM in the two basins. IMERG overestimated low
482 flows for the majority of time in both IMD and TRMM calibrated VIC model for both the
483 basins, and thus was inferior in performance to TRMM. This suggests that the use of an
484 appropriate post-processor (in form of real-time error updation) could tremendously benefit
485 the flow simulations, which might be an interesting study for the future.

486 **4 Conclusions**

487 TRMM 3B42 and IMERG precipitation estimates were comprehensively evaluated over
488 86 basins in India. TRMM 3B42 was analysed for two distinct time periods, the retrospective
489 analysis was carried out from 1998-2013 and the current estimates were compared with
490 IMERG for the year 2014 (March 12th 2014 – December 31st 2014). The systematic biases in
491 both the estimates were explored with respect to a climatologic parameter (basin mean annual
492 rainfall) and a topographic parameter (basin mean elevation). Finally, TRMM and IMERG
493 were hydrologically evaluated by carrying out rainfall-runoff modeling over Hirakud
494 catchment of Mahanadi River basin and Wainganga catchment of Godavari River basin. The
495 results of the study are summarized as:

- 496 1. IMERG rainfall estimates were found to be better than TRMM at all rainfall intensities, in
497 terms of correlation. IMERG outperformed TRMM in 60, 52, 52 and 55 out of 86 basins
498 for overall, low, medium and high rainfall regimes.
- 499 2. IMERG gave better estimates of low rainfall magnitudes with smaller biases in 75 out of
500 the 86 basins analysed, which suggests that the sensor improvement in IMERG satellite

501 translated into better low rainfall estimation. IMERG captured the low rainfall
502 magnitudes better over the Indo-Gangetic plain, North Eastern basins of Brahmaputra and
503 Barak, Central India (Mahi, Chambal and the Indo-Gangetic plain) and the rain shadow
504 area of the Western Ghats. However, for the semi-arid North Western basins, TRMM low
505 rainfall estimates outperformed IMERG.

- 506 3. The high rainfall estimates of IMERG outperformed TRMM in the rain-shadow area of
507 the Western Ghats, the high elevation basins of the North and the South-Eastern basins of
508 Pennar and Cauvery. However, TRMM did a better job in the North-Eastern basins of
509 Brahmaputra and Barak and the North-Western basins of Rajasthan.
- 510 4. Increasing rainfall thresholds lead to deteriorating trends in POD and FAR across
511 majority of basins, with decreasing POD and increasing FAR.
- 512 5. The skill of TRMM-R medium rainfall estimates (in terms of Pbias and correlation) was
513 found to exhibit strong systematic dependence on annual rainfall (climatologic
514 parameter), with larger bias and lower correlation in basins which received higher annual
515 rainfall. This systematic dependence was reduced significantly in IMERG estimates.
516 However, no such improvement was found at low and high rainfall intensities.
- 517 6. A very strong deteriorating skill (increasing bias and decreasing correlation) was found in
518 TRMM-R rainfall estimates at all intensities in the high elevation basins. This systematic
519 dependence was strongly reduced in IMERG estimates at all rainfall intensities,
520 suggesting IMERG captures the rainfall trends better with respect to topography.
- 521 7. Rainfall runoff modeling using VIC model over Mahanadi and Wainganga River basins
522 gave better results with TRMM as input forcing, rather than IMERG. Both TRMM and
523 IMERG captured the phase of the peak flows, however both underreported the
524 magnitudes. Low flows were grossly over predicted by IMERG, which led to overall poor
525 performance with IMERG. As GPM is still a young mission, with time a longer
526 timeseries of IMERG will help in model evaluation as IMERG can be used to directly
527 calibrate the model, hence capturing the fine details in the product.

528 In essence, IMERG gives reasonable improvement in rainfall estimates across majority of
529 the Indian basins. The most notable improvement in IMERG is the reduction in systematic
530 error dependence on topography (basin mean elevation), which suggests improvements in the
531 assimilation of satellite observations. The improved sensitivity of Ku and Ka bands in GPM
532 satellite resulted in improvement in detection of low rainfall magnitudes. The expected
533 improvement in IMERG in snow detection could not be verified in this study as India is

534 mostly a tropical country which receives very less snow. The constant overestimation of low
535 flow magnitudes in the rainfall-runoff exercise suggest that IMERG may benefit from a post
536 forecast data assimilation scheme, which is a worthy topic for further research.

537 **References**

- 538 Akhtar, M. K., Corzo, G. A., van Andel, S. J. and Jonoski, A.: River flow forecasting with
539 artificial neural networks using satellite observed precipitation pre-processed with flow
540 length and travel time information: case study of the Ganges river basin, *Hydrol. Earth Syst.*
541 *Sci.*, 13(9), 1607–1618, doi:10.5194/hess-13-1607-2009, 2009.
- 542 Artan, G., Gadain, H., Smith, J. L., Asante, K., Bandaragoda, C. J. and Verdin, J. P.:
543 Adequacy of satellite derived rainfall data for stream flow modeling, *Nat. Hazards*, 43, 167–
544 185, doi:10.1007/s11069-007-9121-6, 2007.
- 545 Bajracharya, S. R., Shrestha, M. S. and Shrestha, A. B.: Assessment of high-resolution
546 satellite rainfall estimation products in a streamflow model for flood prediction in the
547 Bagmati basin, Nepal, *J. Flood Risk Manag.*, 1–12, doi:10.1111/jfr3.12133, 2014.
- 548 Bisht, D. S., Chatterjee, C., Raghuwanshi, N. S. and Sridhar, V.: Spatio-temporal trends of
549 rainfall across Indian river basins, *Theor. Appl. Climatol.*, 1–18, doi:10.1007/s00704-017-
550 2095-8, 2017.
- 551 Collischonn, B., Collischonn, W. and Tucci, C. E. M.: Daily hydrological modeling in the
552 Amazon basin using TRMM rainfall estimates, *J. Hydrol.*, 360, 207–216,
553 doi:10.1016/j.jhydrol.2008.07.032, 2008.
- 554 Duband, D., Obled, C. and Rodriguez, J. Y.: Unit hydrograph revisited: an alternate iterative
555 approach to UH and effective precipitation identification, *J. Hydrol.*, 150(1), 115–149,
556 doi:10.1016/0022-1694(93)90158-6, 1993.
- 557 Gao, Y. C. and Liu, M. F.: Evaluation of high-resolution satellite precipitation products using
558 rain gauge observations over the Tibetan Plateau, *Hydrol. Earth Syst. Sci.*, 17(2), 837–849,
559 doi:10.5194/hess-17-837-2013, 2013.
- 560 Hamlet, A. F. and Lettenmaier, D. P.: Columbia River Streamflow Forecasting Based on
561 ENSO and PDO Climate Signals, *J. Water Resour. Plan. Manag.*, 125(6), 333–341,
562 doi:10.1061/(ASCE)0733-9496(1999)125:6(333), 1999.
- 563 Hou, A. Y., Kakar, R. K., Neeck, S., Azarbarzin, A. A., Kummerow, C. D., Kojima, M., Oki,
564 R., Nakamura, K. and Iguchi, T.: The Global Precipitation Measurement Mission, *Bull. Am.*
565 *Meteorol. Soc.*, 95(5), 701–722, doi:10.1175/BAMS-D-13-00164.1, 2014.

566 Huffman, G. J., Bolvin, D. T., Nelkin, E. J., Wolff, D. B., Adler, R. F., Gu, G., Hong, Y.,
567 Bowman, K. P. and Stocker, E. F.: The TRMM Multisatellite Precipitation Analysis (TMPA):
568 Quasi-Global, Multiyear, Combined-Sensor Precipitation Estimates at Fine Scales, *J.*
569 *Hydrometeorol.*, 8(1), 38–55, doi:10.1175/JHM560.1, 2007.

570 Huffman, G. J., Bolvin, D. T. and Nelkin, E. J.: Integrated Multi-satellitE Retrievals for GPM
571 (IMERG) Technical Documentation, 2014.

572 India, G. of: Watershed Atlas of India. [online] Available from: [http://india-](http://india-wris.nrsc.gov.in/Publications/WatershedSubbasinAtlas/Watershed%20Atlas%20of%20India.pdf)
573 [wris.nrsc.gov.in/Publications/WatershedSubbasinAtlas/Watershed Atlas of India.pdf](http://india-wris.nrsc.gov.in/Publications/WatershedSubbasinAtlas/Watershed Atlas of India.pdf), 2014.

574 Jena, P. P., Chatterjee, C., Pradhan, G. and Mishra, A.: Are recent frequent high floods in
575 Mahanadi basin in eastern India due to increase in extreme rainfalls?, *J. Hydrol.*, 517, 847–
576 862, doi:10.1016/j.jhydrol.2014.06.021, 2014.

577 Kneis, D., Chatterjee, C. and Singh, R.: Evaluation of TRMM rainfall estimates over a large
578 Indian river basin (Mahanadi), *Hydrol. Earth Syst. Sci.*, 18(7), 2493–2502 [online] Available
579 from: <http://www.hydrol-earth-syst-sci-discuss.net/11/1169/2014/hessd-11-1169-2014.pdf>
580 (Accessed 20 October 2014), 2014.

581 Liang, X., Lettenmaier, D. P., Wood, E. F. and Burges, S. J.: A simple hydrologically based
582 model of land surface water and energy fluxes for general circulation models, *J. Geophys.*
583 *Res.*, 99(D7), 14415, doi:10.1029/94JD00483, 1994.

584 Liang, X., Wood, E. F. and Lettenmaier, D. P.: Surface soil moisture parameterization of the
585 VIC-2L model: Evaluation and modification, *Glob. Planet. Change*, 13, 195–206,
586 doi:10.1016/0921-8181(95)00046-1, 1996.

587 Liu, Z.: Comparison of Integrated Multi-satellitE Retrievals for GPM (IMERG) and TRMM
588 Multi-satellite Precipitation Analysis (TMPA) Monthly Precipitation Products: Initial
589 Results, *J. Hydrometeorol.*, 17, 777–790, doi:10.1175/JHM-D-15-0068.1, 2016.

590 Lohmann, D., Nolte-Holube, R. and Raschke, E.: A large-scale horizontal routing model to
591 be coupled to land surface parametrization schemes, *Tellus A*, 48(5), 708–721,
592 doi:10.1034/j.1600-0870.1996.t01-3-00009.x, 1996.

593 McCuen, R. H.: Assessment of Hydrological and Statistical Significance, *J. Hydrol. Eng.*,
594 21(4), 2516001, doi:10.1061/(ASCE)HE.1943-5584.0001340, 2016.

595 Melsen, L. A., Teuling, A. J., Torfs, P. J. J. F., Uijlenhoet, R., Mizukami, N. and Clark, M.
596 P.: HESS Opinions: The need for process-based evaluation of large-domain hyper-resolution
597 models, *Hydrol. Earth Syst. Sci.*, 20(3), 1069–1079, doi:10.5194/hess-20-1069-2016, 2016.

598 Mujumdar, P. P.: Share data on water resources, *Nature*, 521(7551), 151–152, 2015.

599 Pai, D. S., Sridhar, L., Rajeevan, M., Sreejith, O. P., Satbhai, N. S. and Mukhopadhyay, B.:
600 Development of a new high spatial resolution (0.25× 0.25) long period (1901–2010) daily
601 gridded rainfall data set over India and its comparison with existing data sets over the region.,
602 *Mausam*, 65(1), 1–18, 2014.

603 Peng, B., Shi, J., Ni-Meister, W., Zhao, T. and Ji, D.: Evaluation of TRMM Multisatellite
604 Precipitation Analysis (TMPA) Products and Their Potential Hydrological Application at an
605 Arid and Semiarid Basin in China, *IEEE J. Sel. Top. Appl. Earth Obs. Remote Sens.*, 7(9),
606 3915–3930, doi:10.1109/JSTARS.2014.2320756, 2014.

607 Prakash, S., Mitra, A. K., Momin, I. M., Gairola, R. M., Pai, D. S., Rajagopal, E. N. and
608 Basu, S.: A review of recent evaluations of TRMM Multisatellite Precipitation Analysis
609 (TMPA) research products against ground-based observations over Indian land and oceanic
610 regions, *MAUSAM*, 66(3), 355–366 [online] Available from:
611 [https://www.researchgate.net/profile/Satya_Prakash/publication/281115874_A_review_of_re](https://www.researchgate.net/profile/Satya_Prakash/publication/281115874_A_review_of_recent_evaluations_of_TRMM_Multisatellite_Precipitation_Analysis_(TMPA)_research_products_against_ground-based_observations_over_Indian_land_and_oceanic_regions/links/55e)
612 [cent_evaluations_of_TRMM_Multisatellite_Precipitation_Analysis_\(TMPA\)_research_prod](https://www.researchgate.net/profile/Satya_Prakash/publication/281115874_A_review_of_recent_evaluations_of_TRMM_Multisatellite_Precipitation_Analysis_(TMPA)_research_products_against_ground-based_observations_over_Indian_land_and_oceanic_regions/links/55e)
613 [ucts_against_ground-based_observations_over_Indian_land_and_oceanic_regions/links/55e](https://www.researchgate.net/profile/Satya_Prakash/publication/281115874_A_review_of_recent_evaluations_of_TRMM_Multisatellite_Precipitation_Analysis_(TMPA)_research_products_against_ground-based_observations_over_Indian_land_and_oceanic_regions/links/55e),
614 2015.

615 Prakash, S., Mitra, A. K., AghaKouchak, A., Liu, Z., Norouzi, H. and Pai, D. S.: A
616 preliminary assessment of GPM-based multi-satellite precipitation estimates over a monsoon
617 dominated region, *J. Hydrol.*, doi:10.1016/j.jhydrol.2016.01.029, 2016a.

618 Prakash, S., Mitra, A. K., Pai, D. S. and AghaKouchak, A.: From TRMM to GPM: How well
619 can heavy rainfall be detected from space?, *Adv. Water Resour.*, 88, 1–7,
620 doi:10.1016/j.advwatres.2015.11.008, 2016b.

621 Shah, H. L. and Mishra, V.: Uncertainty and Bias in Satellite-based Precipitation Estimates
622 over Indian Sub-continental Basins: Implications for Real-time Streamflow Simulation and
623 Flood Prediction, *J. Hydrometeorol.*, 17(2), 615–636, doi:10.1175/JHM-D-15-0115.1, 2016.

624 Srivastava, A. K., Rajeevan, M. and Kshirsagar, S. R.: Development of a high resolution

625 daily gridded temperature data set (1969-2005) for the Indian region, *Atmos. Sci. Lett.*, 10(4),
626 249–254, doi:10.1002/asl.232, 2009.

627 Tang, G., Ma, Y., Long, D., Zhong, L. and Hong, Y.: Evaluation of GPM Day-1 IMERG and
628 TMPA Version-7 legacy products over Mainland China at multiple spatiotemporal scales, *J.*
629 *Hydrol.*, 533, 152–167, doi:10.1016/j.jhydrol.2015.12.008, 2016a.

630 Tang, G., Zeng, Z., Long, D., Guo, X., Yong, B., Zhang, W. and Hong, Y.: Statistical and
631 Hydrological Comparisons between TRMM and GPM Level-3 Products over a Midlatitude
632 Basin: Is Day-1 IMERG a Good Successor for TMPA 3B42V7?, *J. Hydrometeorol.*, 17(1),
633 121–137, doi:10.1175/JHM-D-15-0059.1, 2016b.

634 Tawde, S. A. and Singh, C.: Investigation of orographic features influencing spatial
635 distribution of rainfall over the Western Ghats of India using satellite data, *Int. J. Climatol.*,
636 35(9), 2280–2293, doi:10.1002/joc.4146, 2015.

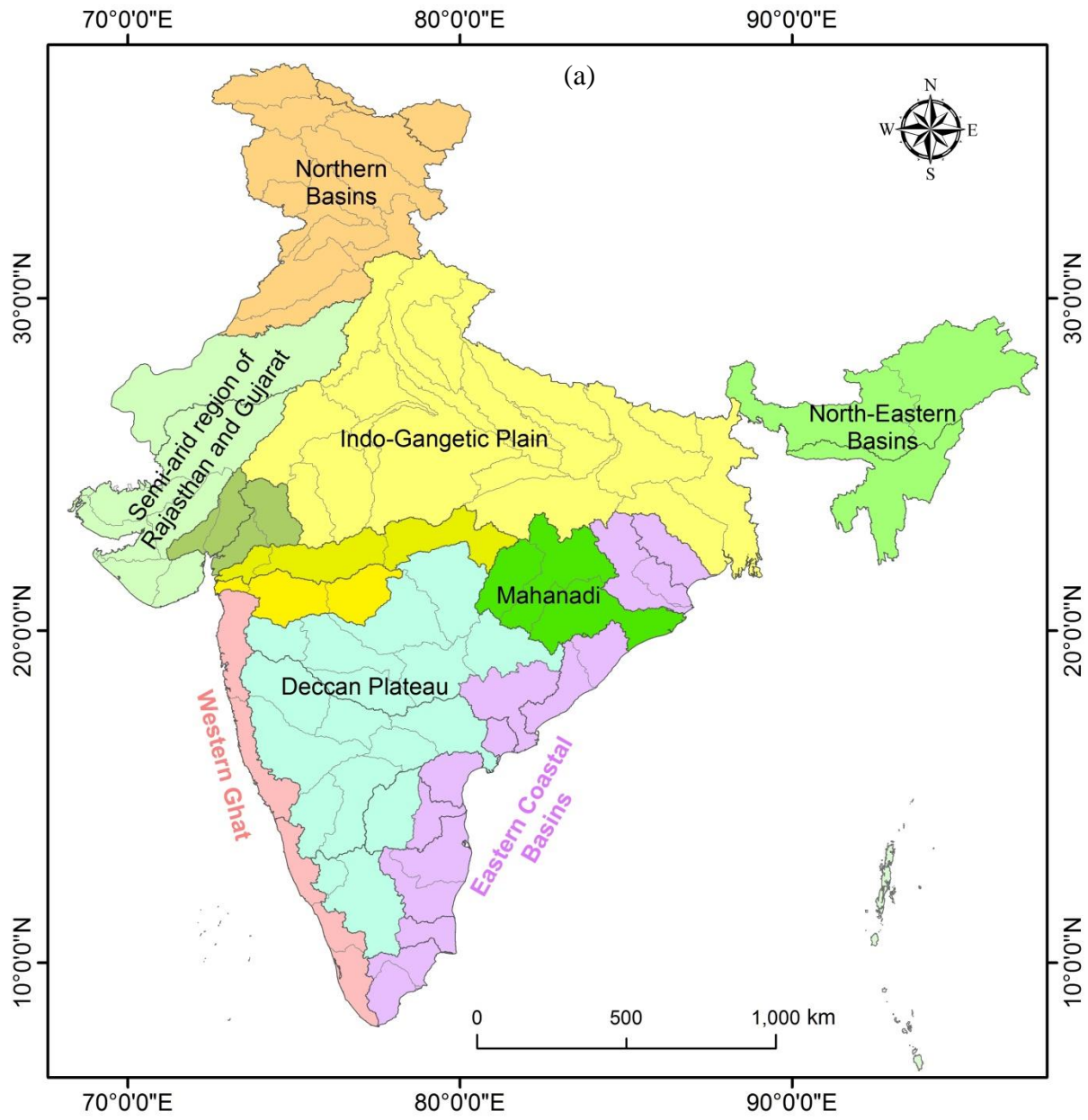
637 Tong, K., Su, F., Yang, D. and Hao, Z.: Evaluation of satellite precipitation retrievals and
638 their potential utilities in hydrologic modeling over the Tibetan Plateau, *J. Hydrol.*, 519, 423–
639 437, doi:10.1016/j.jhydrol.2014.07.044, 2014.

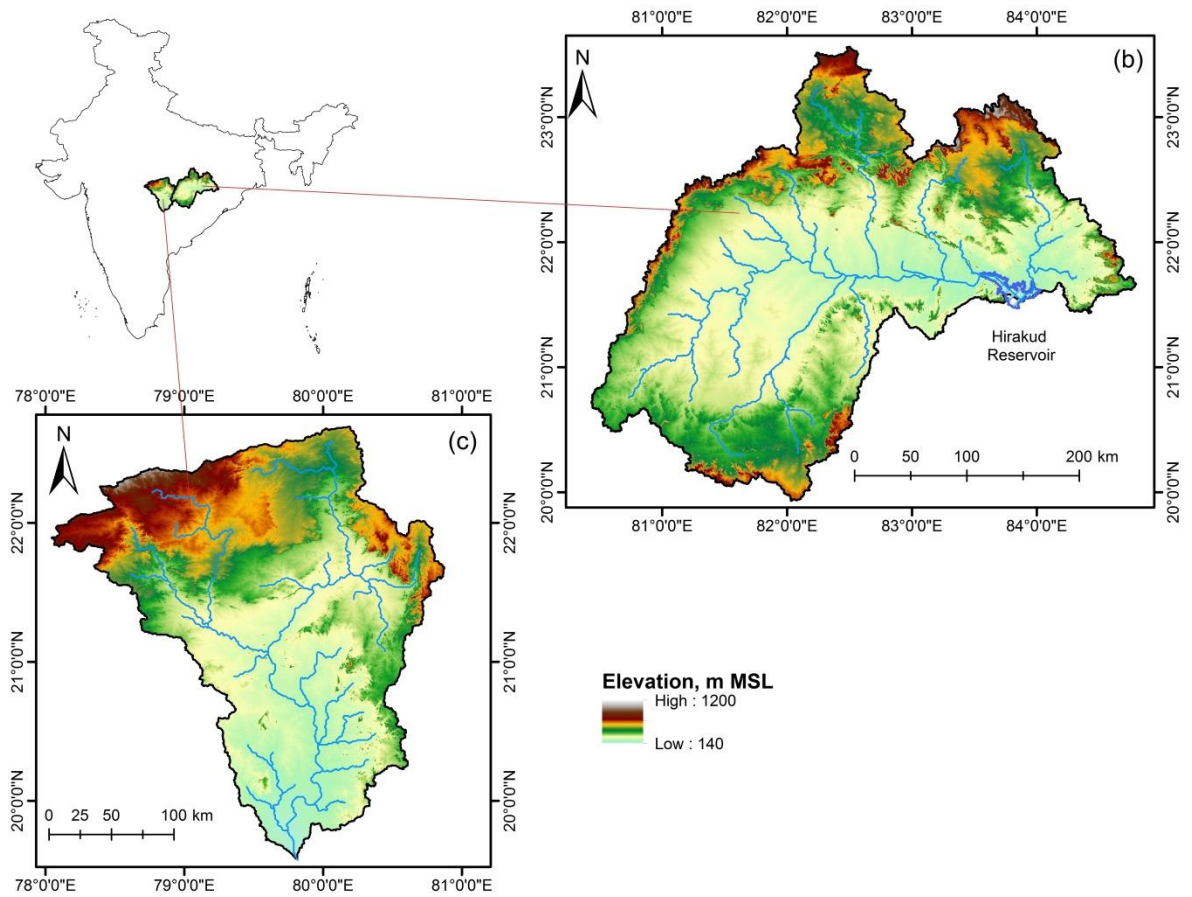
640 Wu, H., Adler, R. F., Hong, Y., Tian, Y. and Policelli, F.: Evaluation of Global Flood
641 Detection Using Satellite-Based Rainfall and a Hydrologic Model, *J. Hydrometeorol.*, 13(4),
642 1268–1284, doi:10.1175/JHM-D-11-087.1, 2012.

643 Wu, X., Xiang, X., Li, L. and Wang, C.: Water level updating model for flow calculation of
644 river networks, *Water Sci. Eng.*, 7(1), 60–69, doi:10.3882/j.issn.1674-2370.2014.01.007,
645 2014.

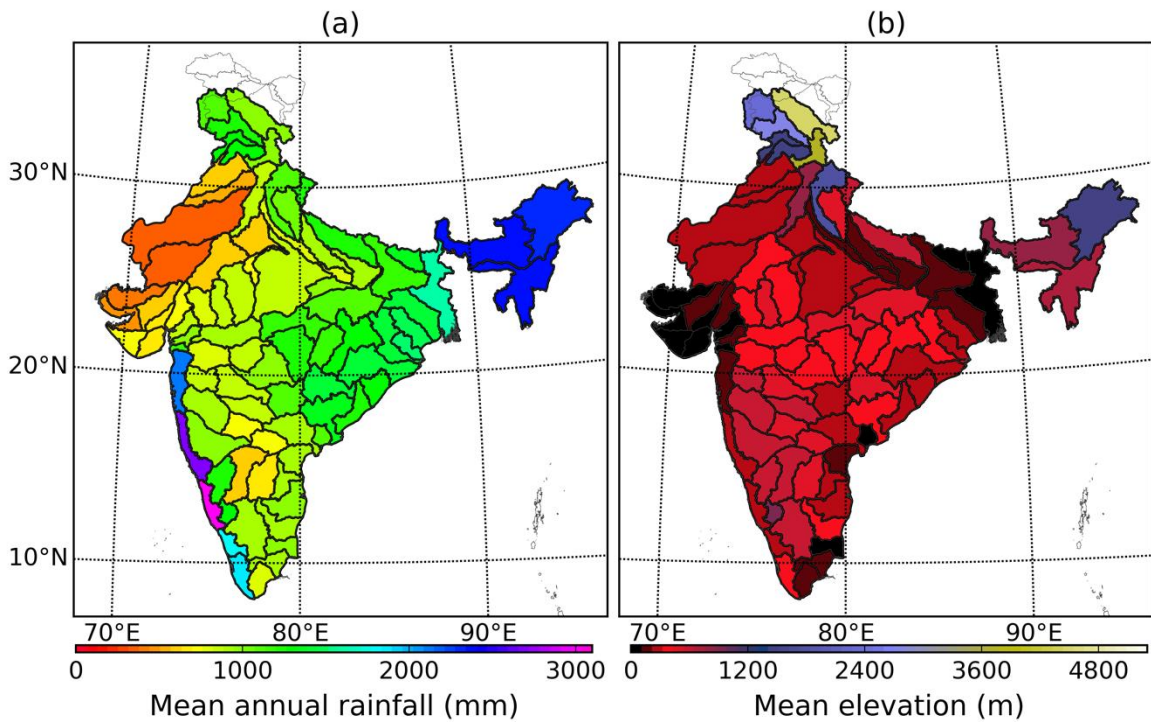
646 Yong, B., Hong, Y., Ren, L.-L., Gourley, J. J., Huffman, G. J., Chen, X., Wang, W. and
647 Khan, S. I.: Assessment of evolving TRMM-based multisatellite real-time precipitation
648 estimation methods and their impacts on hydrologic prediction in a high latitude basin, *J.*
649 *Geophys. Res.*, 117(D9), doi:10.1029/2011JD017069, 2012.

650 Zhu, Q., Xuan, W., Liu, L. and Xu, Y.: Evaluation and hydrological application of
651 precipitation estimates derived from PERSIANN CDR, TRMM 3B42V7 and NCEP CFSR
652 over humid regions in China, *Hydrol. Process.*, 30(17), 3061–3083, doi:10.1002/hyp.10846,
653 2016.



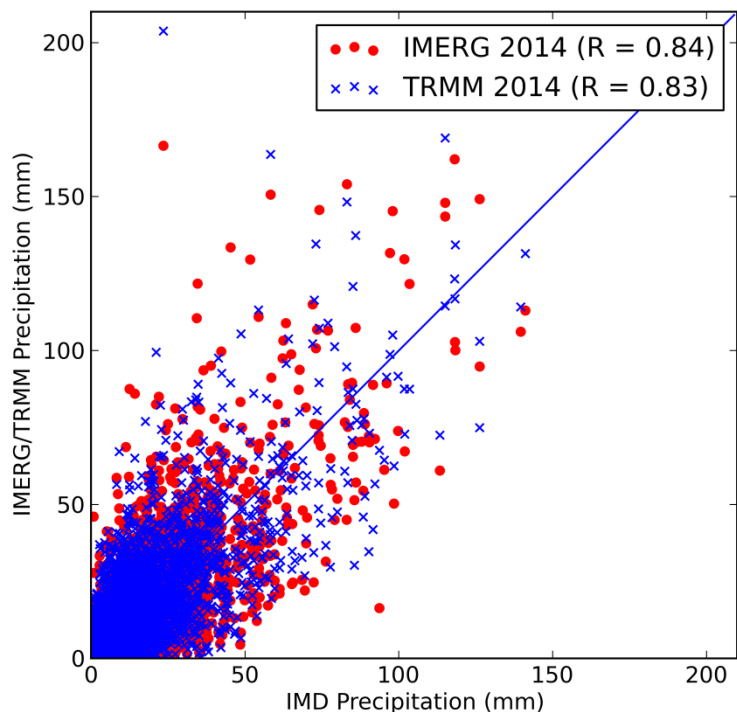


658
 659 **Figure 1(a).** Map of the major basins in India, map of (b) Hirkud catchment of the
 660 Mahanadi River basin and (c) Wainganga catchment of the Godavari River basin.

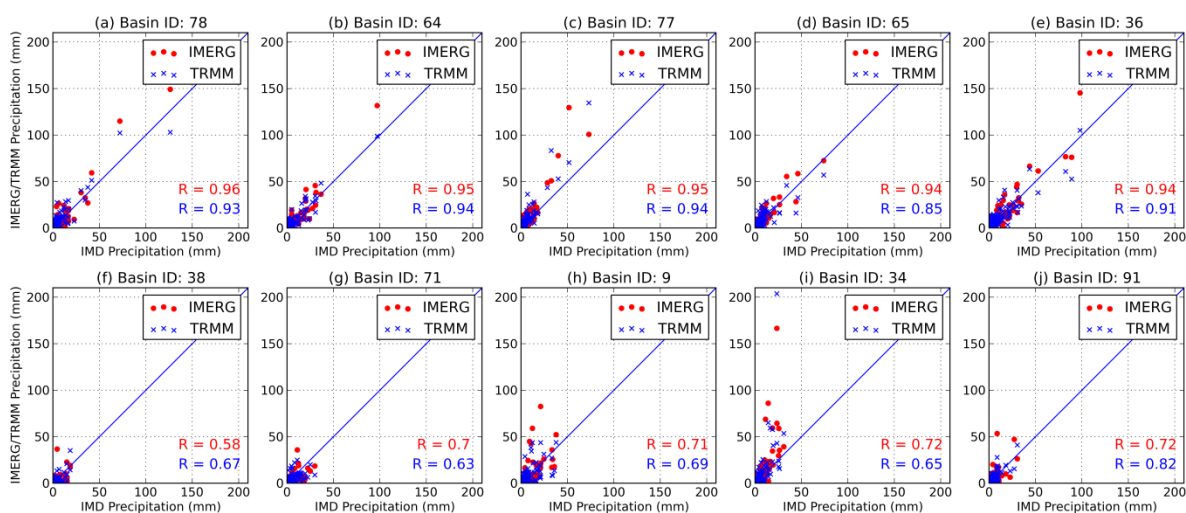


661

662 **Figure 2.** Spatial distribution of (a) long term average annual rainfall (calculated from IMD
 663 gridded rainfall dataset from years 1980-2010), and (b) average elevation above mean sea
 664 level (calculated using SRTM DEM) over 86 major basins in India.

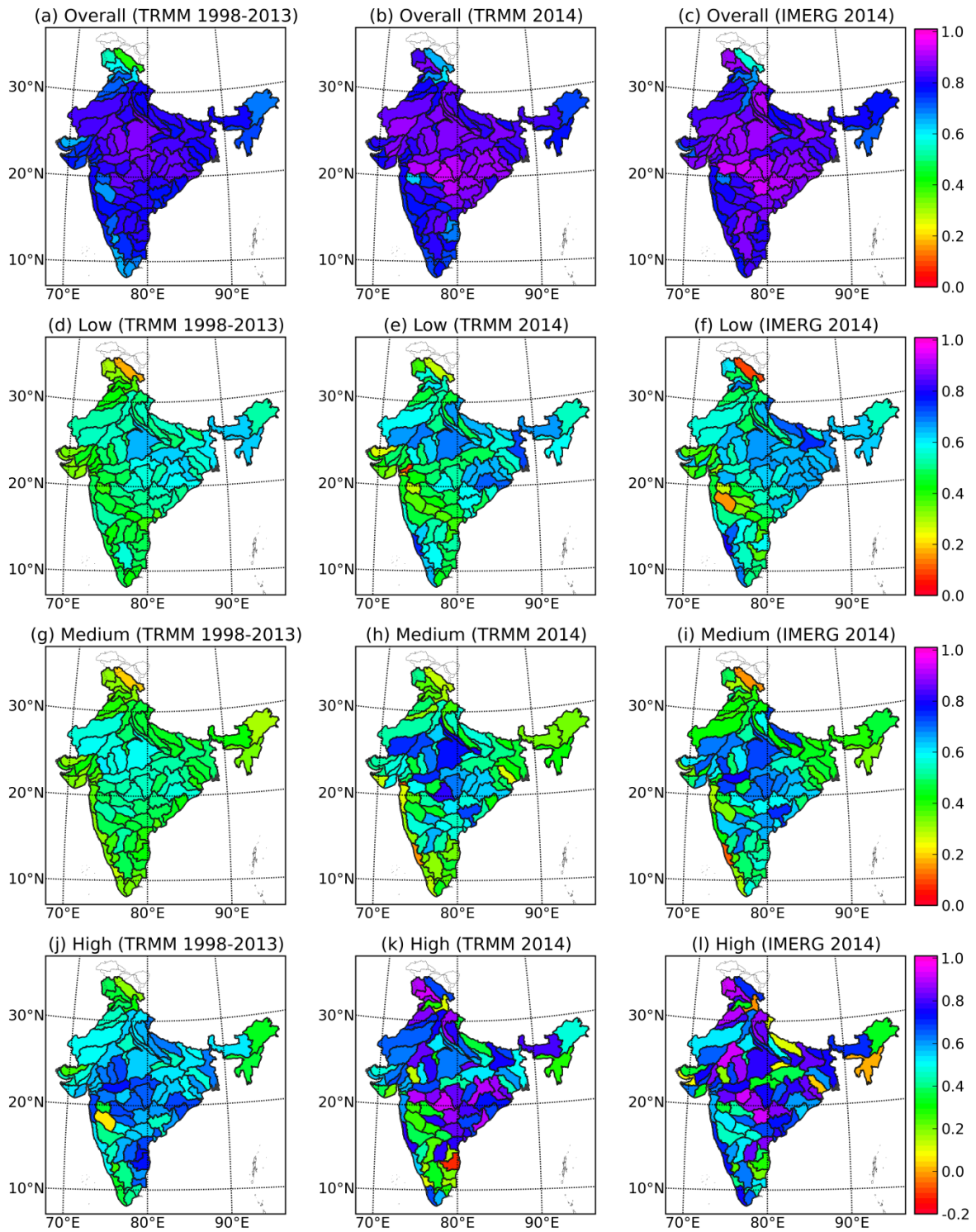


665
 666 **Figure 3.** Scatterplot of satellite precipitation products (TRMM and IMERG) vs observed
 667 rainfall (IMD) computed over 86 major basins in India (based on daily precipitation data
 668 from March 12, 2014 to December 31, 2014).



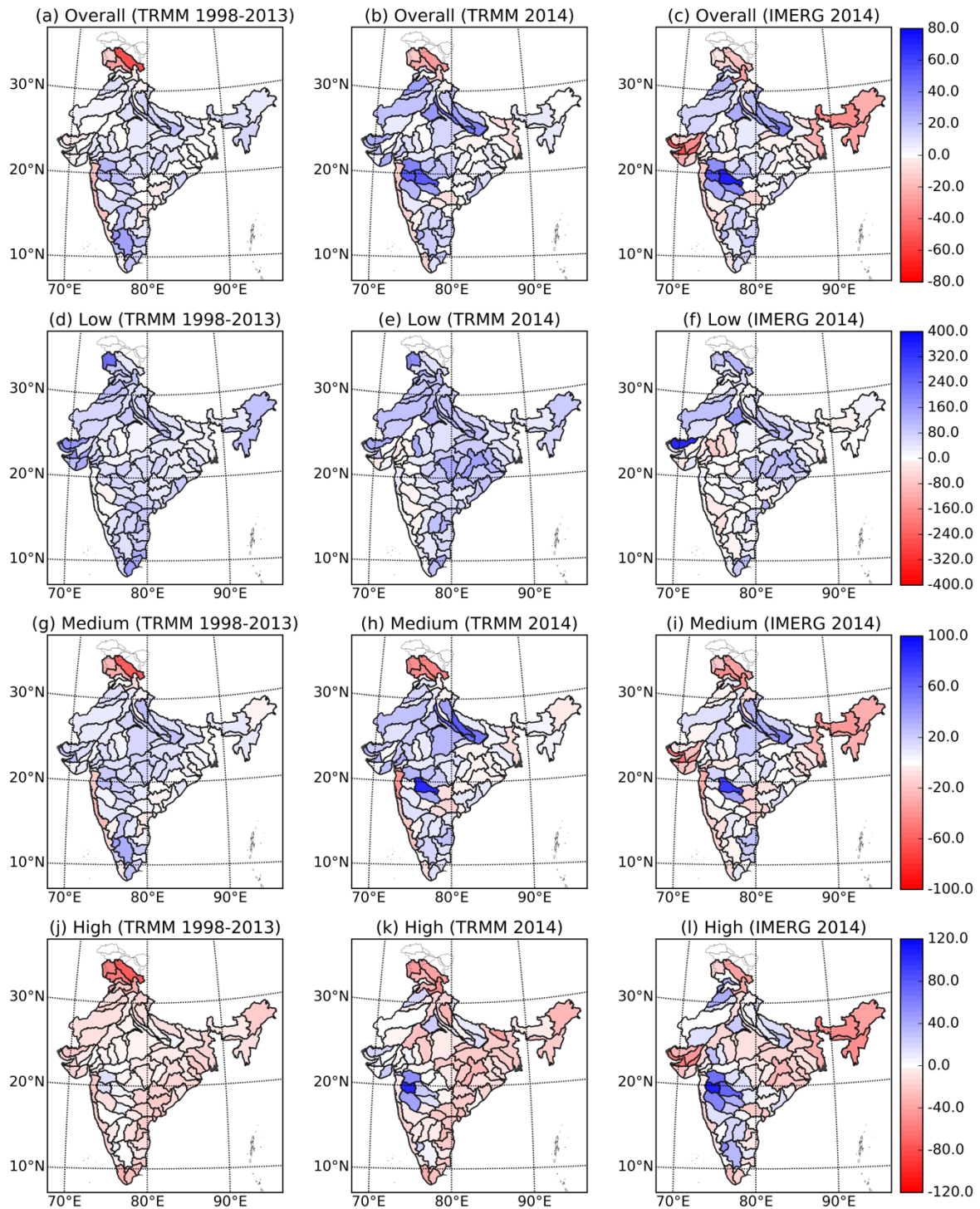
669
 670 **Figure 4.** Scatterplot of satellite precipitation products (TRMM and IMERG) vs observed
 671 rainfall (IMD) for (a) – (e) five best basins in terms of correlation of IMERG with IMD

672 (arranged in descending order) and (f) – (j) five worse basins in terms of correlation of
 673 IMERG with IMD (arranged in ascending order) (based on daily precipitation data from
 674 March 12, 2014 to December 31, 2014).



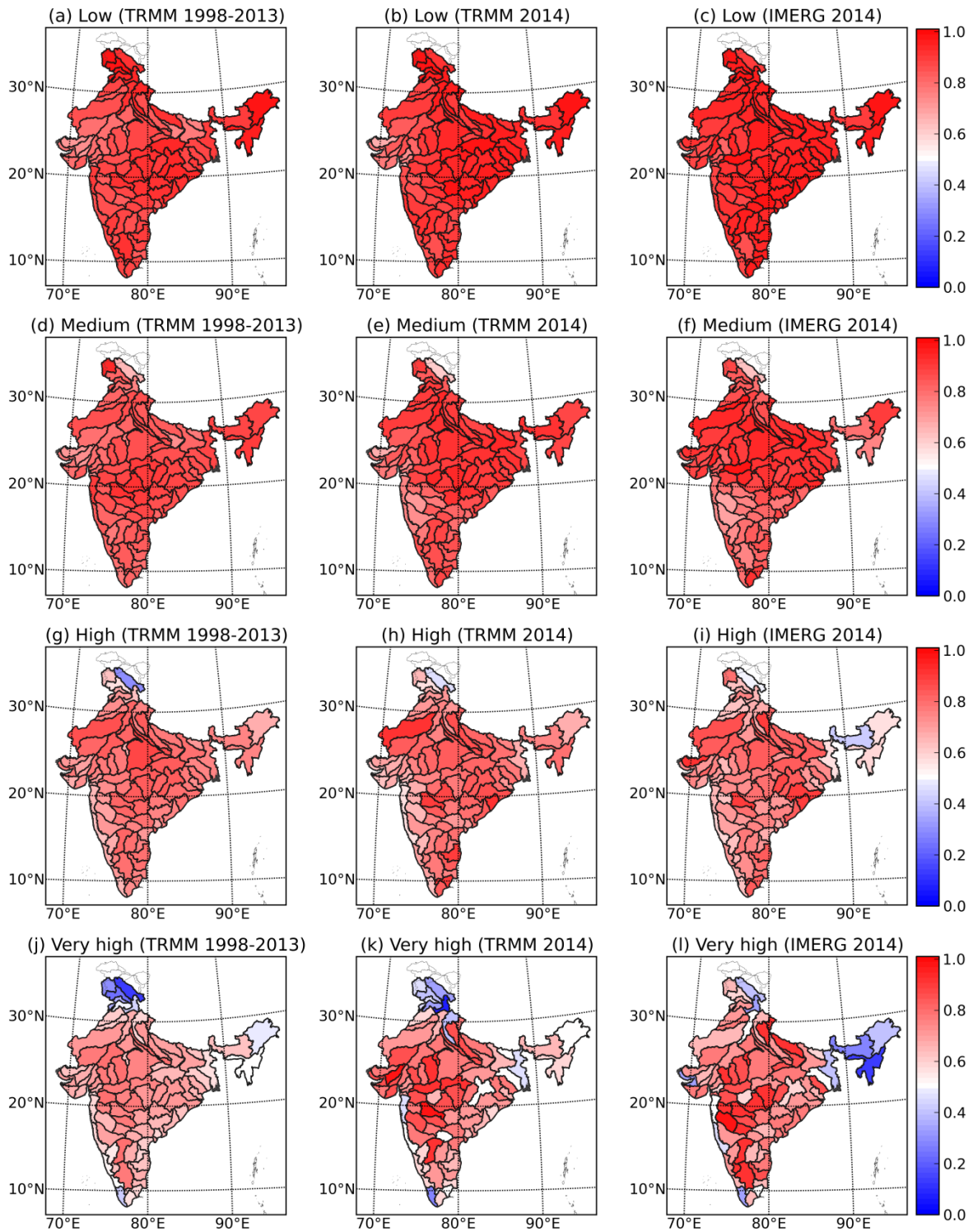
675

676 **Figure 5.** Spatial representation of correlation of TRMM (1998-2013), TRMM (2014) and
 677 IMERG (2014) over 86 major basins in India for (a) – (c) overall time series, (d) – (f) low,
 678 (g) – (i) medium and (j) – (l) high rainfall regime.



679

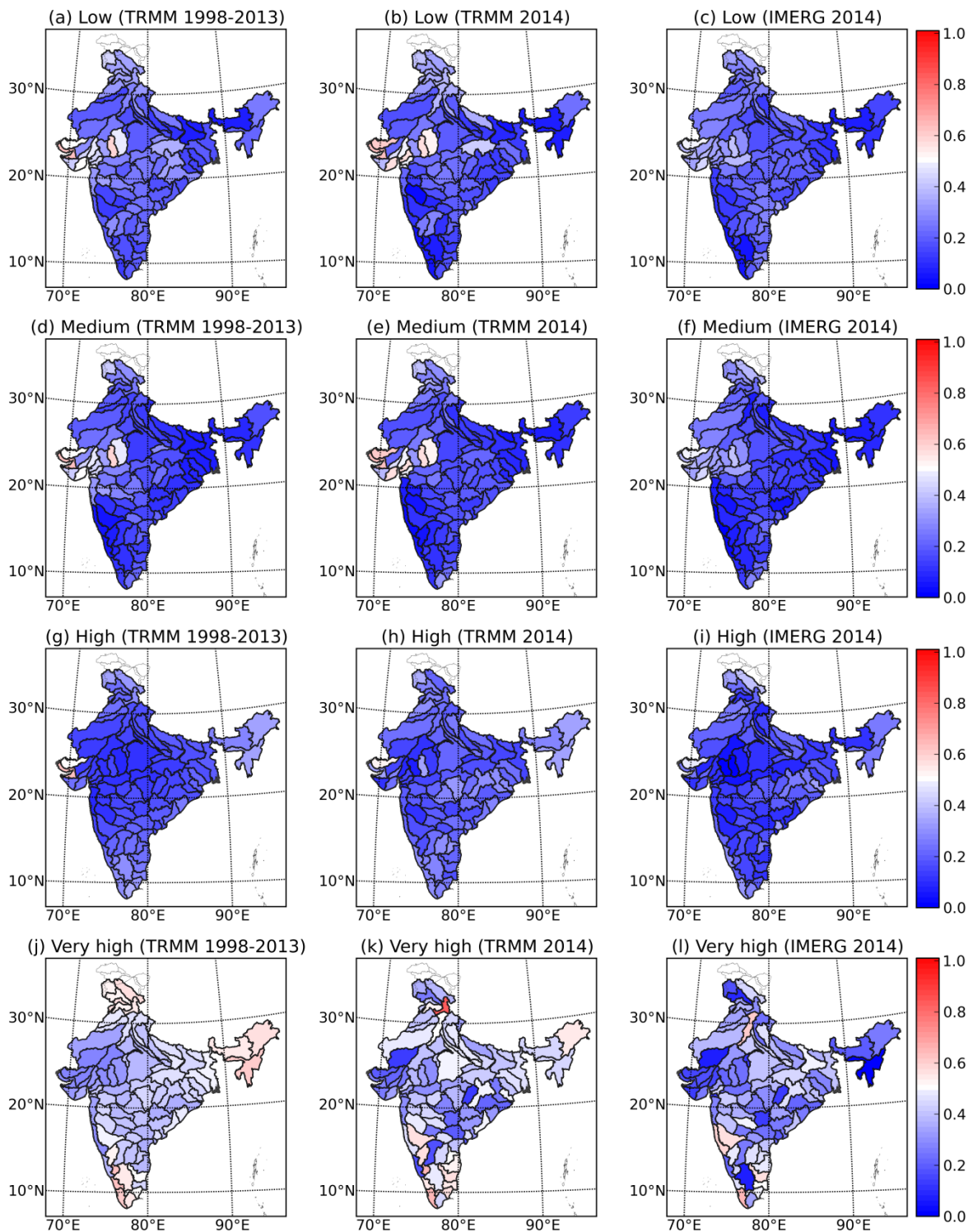
680 **Figure 6.** Spatial representation of percentage bias of TRMM (1998-2013), TRMM (2014)
 681 and IMERG (2014) over 86 major basins in India for (a) – (c) overall time series and over (d)
 682 – (f) low, (g) – (i) medium and (j) – (l) high rainfall regime.



683

684 **Figure 7.** Spatial representation of probability of detection (POD) for (a) – (c) low (25
 685 percentile), (d) – (f) medium (50 percentile), (g) – (i) high (75 percentile) and (j) – (l) very

686 high (95 percentile) rainfall threshold for TRMM (1998-2013), TRMM (2014) and IMERG
 687 (2014) rainfall estimates over 86 major basins in India.

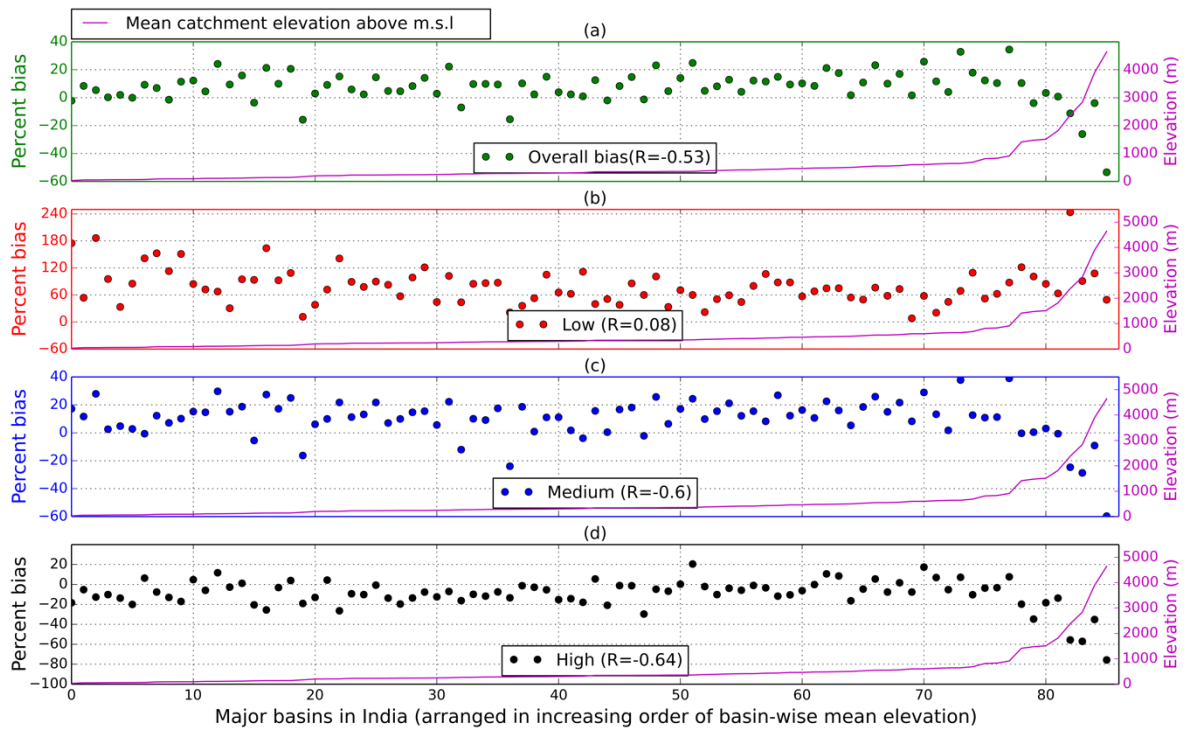


688

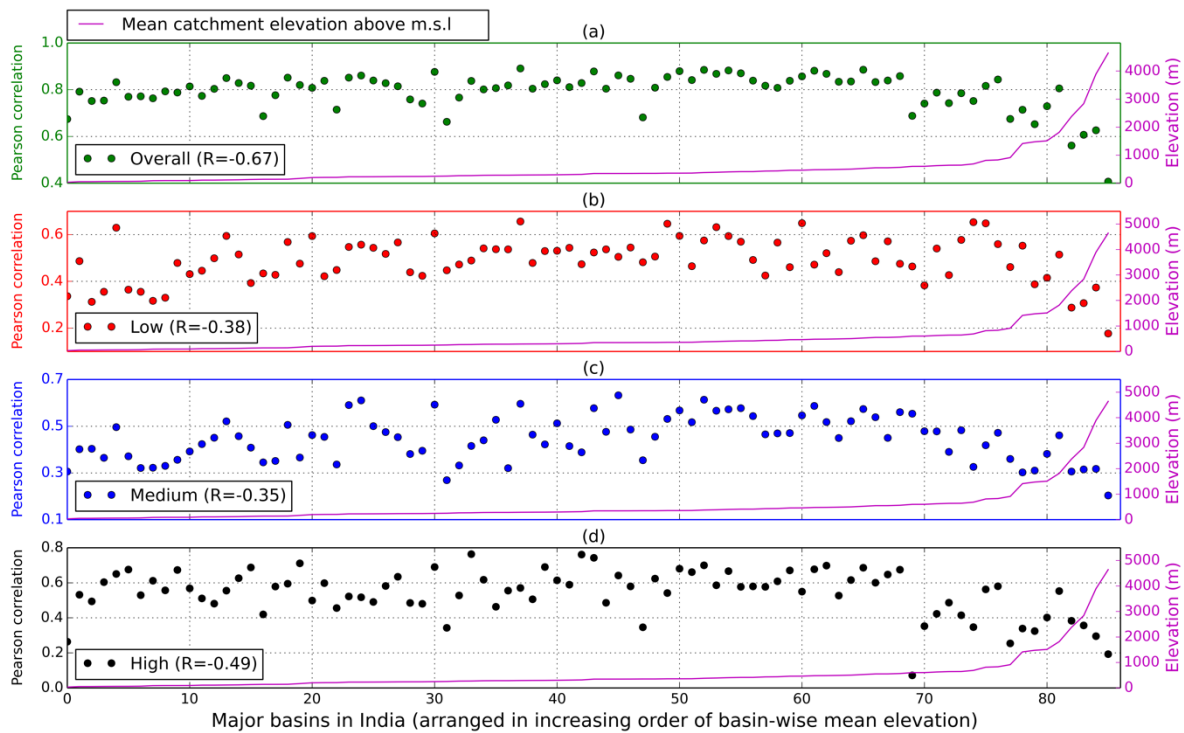
689 **Figure 8.** Spatial representation of false alarm ratio (FAR) for (a) – (c) low (25 percentile),
 690 (d) – (f) medium (50 percentile), (g) – (i) high (75 percentile) and (j) – (l) very high (95

691 percentile) rainfall threshold for TRMM (1998-2013), TRMM (2014) and IMERG (2014)
 692 rainfall estimates over 86 major basins in India.

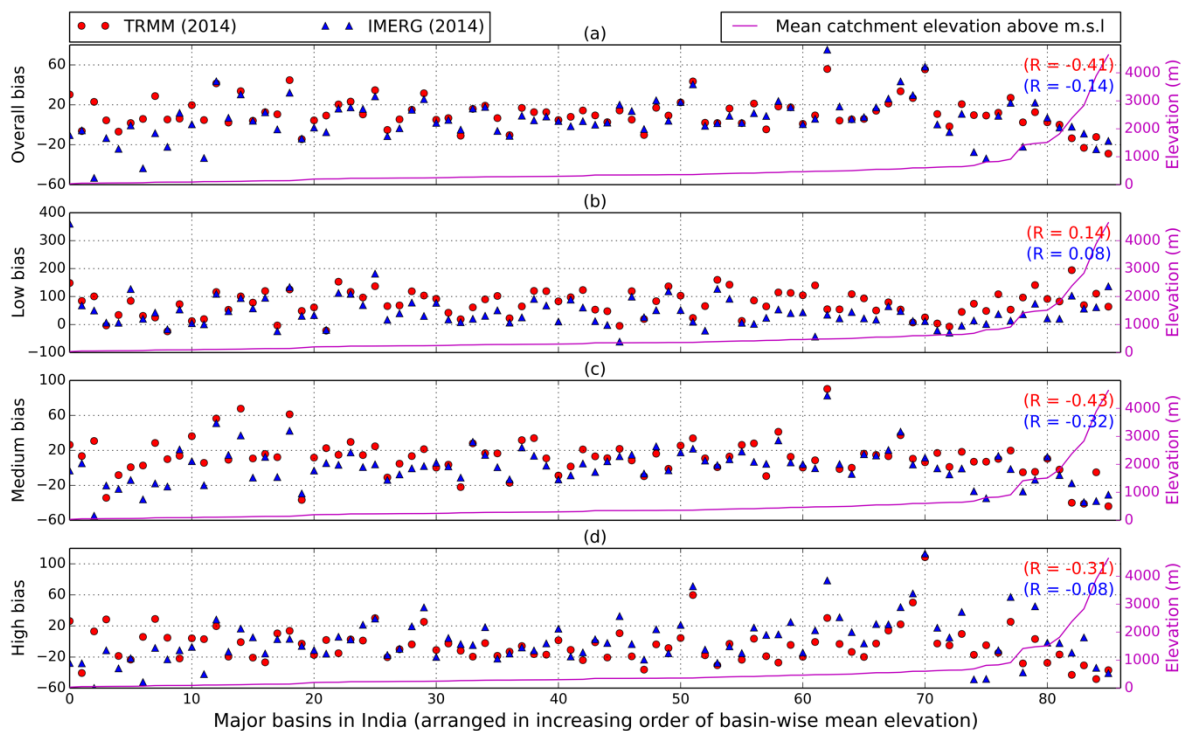
693



694
 695 **Figure 9.** Graphical representation of percentage bias of TRMM (1998-2013) arranged in the
 696 increasing order of basin-wise average elevation over mean sea level for (a) overall time
 697 series and over (b) low, (c) medium and (d) high rainfall regime for 86 major basins in India.

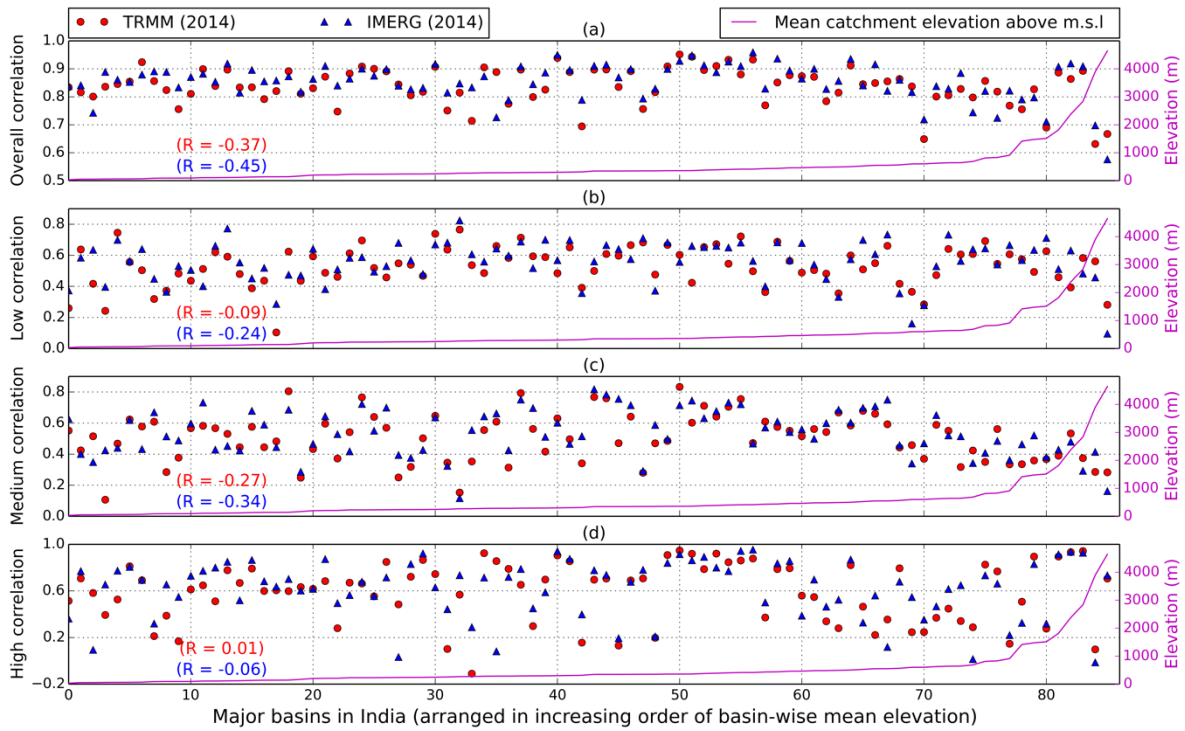


698
 699 **Figure 10.** Graphical representation of correlation of TRMM (1998-2013) arranged in the
 700 increasing order of basin-wise average elevation over mean sea level for (a) overall time
 701 series and over (b) low, (c) medium and (d) high rainfall regime for 86 major basins in India.



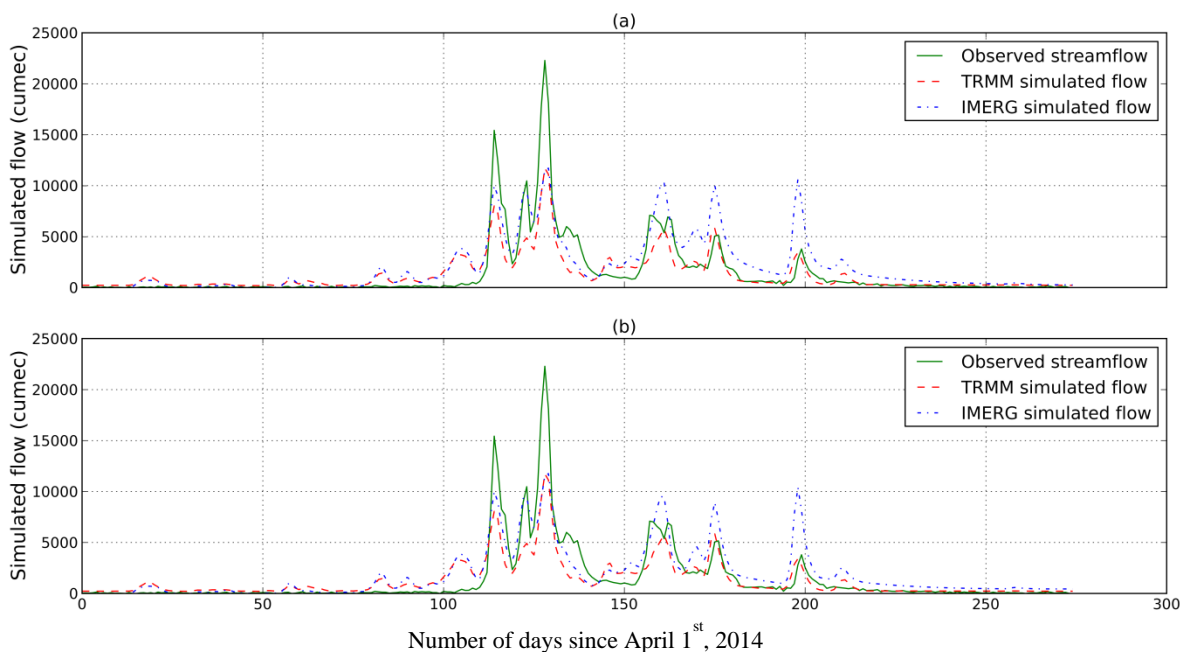
702
 703 **Figure 11.** Graphical representation of percentage bias of IMERG (2014) and TRMM (2014)
 704 arranged in the increasing order of basin-wise average elevation over mean sea level for (a)

705 overall time series and over (b) low, (c) medium and (d) high rainfall regime for 86 major
 706 basins in India.



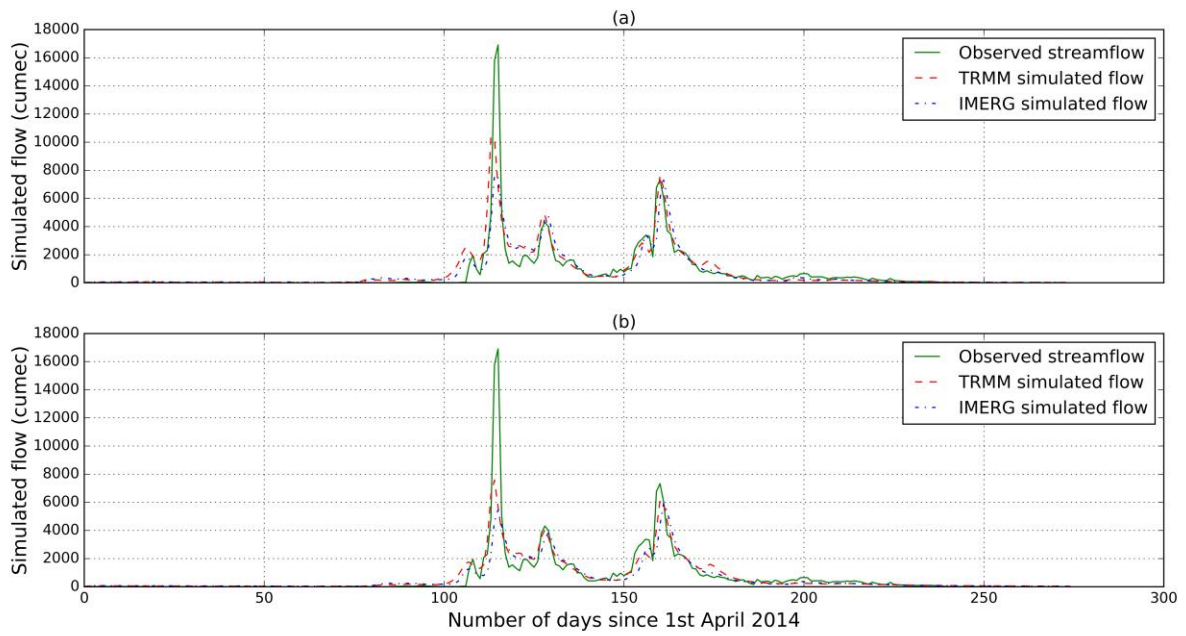
707

708 **Figure 12.** Graphical representation of correlation of IMERG (2014) and TRMM (2014)
 709 arranged in the increasing order of basin-wise average elevation over mean sea level for (a)
 710 overall time series and over (b) low, (c) medium and (d) high rainfall regime for 86 major
 711 basins in India.



712

713 **Figure 13.** Hydrographs for TRMM and IMERG simulations (April 1, 2014 – December 31,
714 2014) with (a) IMD and (b) TRMM calibrated VIC model for Hirakud basin.



715

716 **Figure 14.** Hydrographs for TRMM and IMERG simulations (April 1, 2014 – December 31,
717 2014) with (a) IMD and (b) TRMM calibrated VIC model for Wainganga basin.

718 **Table 1.** Summary of the precipitation datasets used.

Product name	Spatial resolution	Temporal resolution	Spatial coverage	Temporal coverage	Period used in this study
IMD Gridded Rainfall	0.25° x 0.25°	Daily	Indian landmass	1901-2014	1998-2013, 12 th March, 2014 – 31 st December 2014
TRMM Research product	0.25° x 0.25°	3-hourly	50° N-S	1998-present	1998-2013, 12 th March, 2014 – 31 st December 2014
IMERG Final Run	0.1° x 0.1°	Half-hourly	60° N-S	12 th March, 2014 - present	12 th March, 2014 – 31 st December 2014

719 **Table 2.** Contingency table used to calculate probability of detection (POD) and false alarm
 720 ratio (FAR) at a given rainfall threshold.

		Simulated	
		> Threshold	<= Threshold
Observed	> Threshold	HIT	MISS
	<= Threshold	FALSE	NEGATIVE

721 **Table 3.** Summary of different statistical indices used to evaluate the satellite precipitation
 722 products.

Index	Formula	Best value	Worst value
Pearson correlation (R)	$\frac{\sum(X - \bar{X})(Y - \bar{Y})}{\sqrt{\sum(X - \bar{X})^2} \sqrt{\sum(Y - \bar{Y})^2}}$	1	0
Percentage bias (Pbias)	$\frac{\sum(Y - X)}{\sum X} * 100$	0	$+\infty / -\infty$
Probability of detection (POD)	$\frac{HIT}{HIT + MISS}$	1	0
False alarm ratio (FAR)	$\frac{FALSE}{HIT + FALSE}$	0	1
Nash Sutcliffe efficiency (NSE)	$1 - \frac{\sum(X - Y)^2}{\sum(X - \bar{X})^2}$	1	$-\infty$ (negative value means that mean is a better estimator)

			than the model).
Root mean squared error (RMSE)	$\sqrt{\frac{\sum(X - Y)^2}{n}}$	0	$+\infty$

723 ($X = Observed, \bar{X} = Observed\ mean, Y = Simulated, \bar{Y} = Simulated\ mean, n =$
724 $Data\ points$)

725 **Table 4.** Segregation of overall rainfall time series into low, medium and high rainfall time
726 series ($R = Rainfall, \mu = Mean\ of\ rainfall, \sigma = Standard\ deviation\ of\ rainfall$).

Rainfall regime	Criterion
Low	$R < \mu$
Medium	$R \geq \mu$ and $R \leq \mu + 2\sigma$
High	$R > \mu + 2\sigma$

727 **Table 5.** Comparison of the IMERG and TRMM based on the number of basins in which the satellite
728 products show higher/lower correlation based on the year 2014 (R: pearson correlation)

Expression	IMERG	TRMM
$R > 0.8$	73	68
$R > 0.9$	20	13
Higher R	60	26
Higher R (low rainfall regime)	52	34
Higher R (medium rainfall regime)	52	34
Higher R (high rainfall regime)	55	31

729 **Table 6.** Comparison of the IMERG and TRMM based on the number of basins in which the satellite
730 products show higher/lower POD/FAR based on the year 2014. The third column gives the number
731 of basins in which IMERG/TRMM gives similar POD/FAR. (Low, medium, high and very high
732 threshold: 25, 50, 75, 95 percentile respectively)

Expression	IMERG	TRMM	Similar
Higher POD (low rainfall threshold)	62	24	0
Higher POD (medium rainfall threshold)	39	37	10
Higher POD (high rainfall threshold)	32	45	9
Higher POD (very high rainfall threshold)	44	27	15
Lower FAR (low rainfall threshold)	42	40	4
Lower FAR (medium rainfall threshold)	53	26	7
Lower FAR (high rainfall threshold)	67	15	4
Lower FAR (very high rainfall threshold)	64	17	5

733

734

735 **Table 7.** Performance statistics for rainfall-runoff modeling using VIC for Hirakud catchment
 736 of Mahanadi River basin.

	Time period	NSE	R²	P-bias	RMSE (m³/s)
IMD calibration	2000-2011	0.83	0.84	16.78	919.88
IMD validation	2012-2014	0.86	0.88	3.91	823.58
TRMM calibration	2000-2011	0.72	0.74	18.2	1160.94
TRMM validation	2012-2014	0.73	0.74	14	1128.15
TRMM (IMD calibration)	2014	0.72	0.82	-9.41	1591.09
IMERG (IMD calibration)	2014	0.64	0.68	41.4	1786.22
TRMM (TRMM calibration)	2014	0.72	0.82	-9.24	1588.86
IMERG (TRMM calibration)	2014	0.7	0.72	31.32	1641.82

737 **Table 8.** Performance statistics for rainfall-runoff modeling using VIC for Wainganga River
 738 basin.

	Time period	NSE	R² (p-value)	P-bias	RMSE (m³/s)
IMD calibration	2000-2011	0.81	0.81	9.18	740.49
IMD validation	2012-2014	0.87	0.88	-10.8	852.9
TRMM calibration	2000-2011	0.7	0.71	15.66	931.65
TRMM validation	2012-2014	0.83	0.83	5.93	973.41
TRMM (IMD calibration)	2014	0.74	0.74	8.70	883.19
IMERG (IMD calibration)	2014	0.74	0.76	-0.52	883.59
TRMM (TRMM calibration)	2014	0.72	0.75	-2.70	922.04
IMERG (TRMM calibration)	2014	0.61	0.66	-12.10	1082.34

